GASEOUS DISCHARGES AND THEIR APPLICATIONS AS HIGH POWER

PLASMA SWITCHES FOR COMPACT PULSED POWER SYSTEMS

Except where reference is made to the work of others, the work described in this thesis is my own or was done in collaboration with my advisory committee. This thesis does not include proprietary or classified information.

_____
Esin B. Sözer

Certificate of Approval:

_____   _____
Lloyd S. Riggs   Hülya Kirkici, Chair
Professor   Associate Professor
Electrical and Computer Engineering   Electrical and Computer Enginnering

_____   _____
Thaddeus Roppel   George Flowers
Associate Professor   Interim Dean
Electrical and Computer Engineering   Graduate School

GASEOUS DISCHARGES AND THEIR APPLICATIONS AS HIGH POWER

PLASMA SWITCHES FOR COMPACT PULSED POWER SYSTEMS

Esin Bengisu Sözer

A Thesis

Submitted to

the Graduate Faculty of

Auburn University

in Partial Fulfillment of the

Requirements for the

Degree of

Master of Science

Auburn, Alabama
May 10, 2008

GASEOUS DISCHARGES AND THEIR APPLICATIONS AS HIGH POWER

PLASMA SWITCHES FOR COMPACT PULSED POWER SYSTEMS

Esin Bengisu Sözer

Permission is granted to Auburn University to make copies of this thesis at its discretion, upon request of individuals or institutions and at their expense. The author reserves all publication rights.

_____
Signature of Author

_____
Date of Graduation

VITA

Esin Bengisu Sözer, daughter of Dr. E. Emel Sözer and Dr. M. Tekin Sözer, was born on October 28, 1983 in Ankara, Turkey. She graduated from Ankara Ataturk Anatolian High School and joined Hacettepe University, Ankara, Turkey in 2001 for her Bachelors of Science degree in Electronics Engineering. She graduated from Hacettepe University as a Honors student in 2005 and entered Auburn University, Electrical and Computer Engineering Department for her graduate studies.

THESIS ABSTRACT

GASEOUS DISCHARGES AND THEIR APPLICATIONS AS HIGH POWER

PLASMA SWITCHES FOR COMPACT PULSED POWER SYSTEMS

Esin Bengisu Sözer

Master of Science, 10 May 2008
(B.S., Hacettepe University, Ankara, Turkey, 2005)

71 Typed Pages

Directed by Dr. Hülya Kirkici

Today's pulsed power technology requires compact systems for both military and civilian applications, leading to increased demand for research in compact system components. High power switches are one of the fundamental components of all pulsed power systems. Although reliable compact solid-state switches are being reported, their peak energy capabilities are still not sufficient for some high power applications. Therefore, triggered plasma switches with low maintenance and compact design requirements are one of the key research areas. This thesis is a report on gaseous discharges and breakdown processes which are the underlying phenomena in the operation of high power plasma switches and investigation of a possible triggering mechanism for a compact design.

ACKNOWLEDGEMENTS

The author would like to thank her advisor, Dr. Hülya Kirkici, for her guidance during the course of this research. The author also would like to thank Dr. Lloyd S. Riggs and Dr. Thaddeus Roppel for serving in her committee. The author would like to appreciate Linda Barresi and Calvin Cutshaw for material support for the experiments. The author would like to thank fellow graduate student Kalyan Koppisetty for his technical discussions, help and guidance all through the experimental and writing process of this thesis. Thanks are also to all family members, Dr. M. Tekin Sözer, Dr. E. Emel Sözer and Dr. Sevin Sözer-Ertoklar for their lifetime love, support, encouragement and guidance.

Style manual or journal used <u>Auburn University Graduate School: Guide to preparation and submission of theses and dissertations</u>

Computer software used <u>Microsoft Office XP</u>

TABLE OF CONTENTS

LIST OF TABLES

LIST OF FIGURES

CHAPTER 1

INTRODUCTION

1.1   Pulsed Power Engineering

Pulsed Power is the science of storing energy over a long period of time (usually seconds or minutes) and then discharging it as electrical energy over a much shorter period of time (usually microseconds or nanoseconds). In simplest terms, a pulsed power system includes an energy storage stage, a load, and a pulse forming stage between these two stages. The pulse forming stage can be a single high power switch that transfers the stored energy to the load or a more complex system based on a network of high power switches.
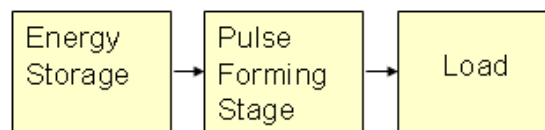
Figure 1 Pulsed power system block diagram

Energy can be stored either inductively or capacitively. In order to transfer inductively stored energy, a high-power opening switch is required to divert the current flow to its parallel branch where the load is connected. The capacitive energy storage

needs a high-power closing switch to transfer the stored energy to the load, which, in this case, is connected in series to the switch. Figure 2 shows basic circuits for these two configurations. These systems can be used together in different configurations to improve the characteristics of the pulse generated, depending on the requirements of the load.

Wide range of pulsed power application areas include materials processing, food processing, medicine and biology. Power sources such as lasers, high power microwave devices, radar modulators, and accelerators for X-ray treatment devices are among the most important applications [1]. Requirements for the pulse length, average and peak energies, and the repetition rate are highly application specific; however, compactness and portability are the common driving forces above these requirements for today's pulsed power systems [2].
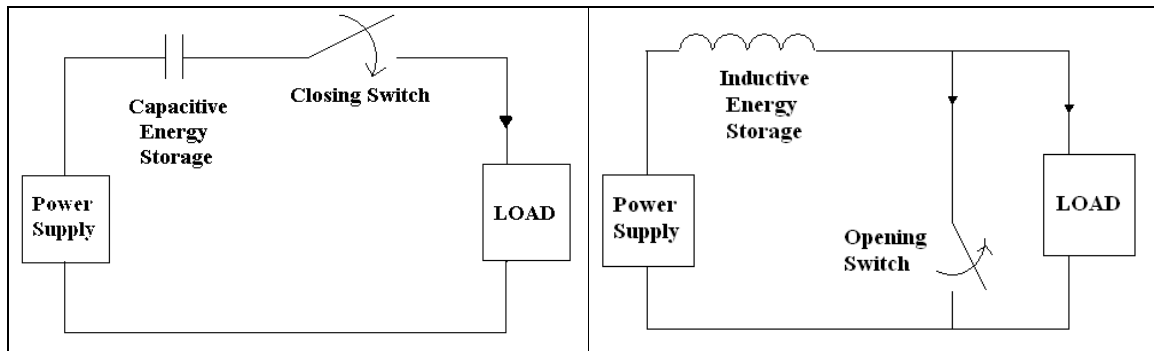
Figure 2 Pulsed Power Circuits with Capacitive and Inductive Energy Storages

1.2 Power Density for Pulsed Power Systems

Mouse-to-elephant curve shown in Figure 3 represents power consumption per unit mass for mammals in biological studies. All mammals fall about a line on a log-log plot of metabolic rate versus body mass since they are composed of similar matter, consume carbon-based food, and breathe oxygen [2].
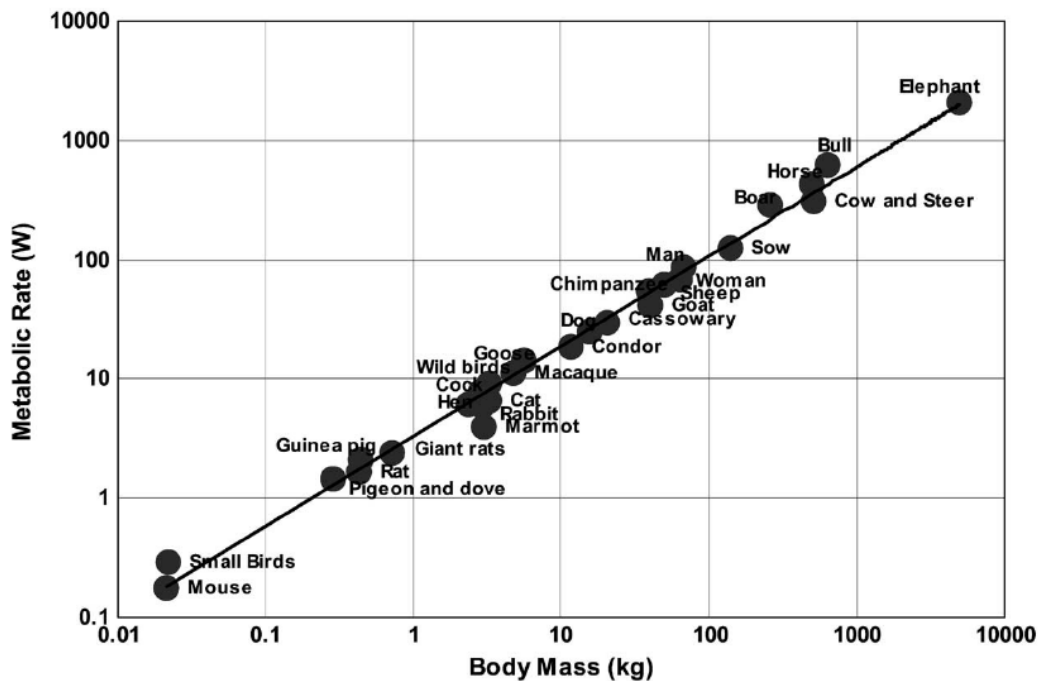
Figure 3 Mouse-to-elephant curve [2]

Figure 4 is an analogy of mouse-to-elephant curve for pulsed power systems where "mouse" is a compact hand-held pulsed power system developed at Los Alamos National Laboratory, Los Alamos, NM, and the "elephant" is the "Z" accelerator at Sandia National Laboratories, Albuquerque, NM, used for high energy density physics research.

Traditional pulsed power systems fall about the lower slope curve because similar to mouse-to-elephant curve; they are composed of similar materials. Today's pulsed power research is driven to develop and incorporate higher power density units for these systems. The line with the higher power density slope represents newer more efficient systems [3].
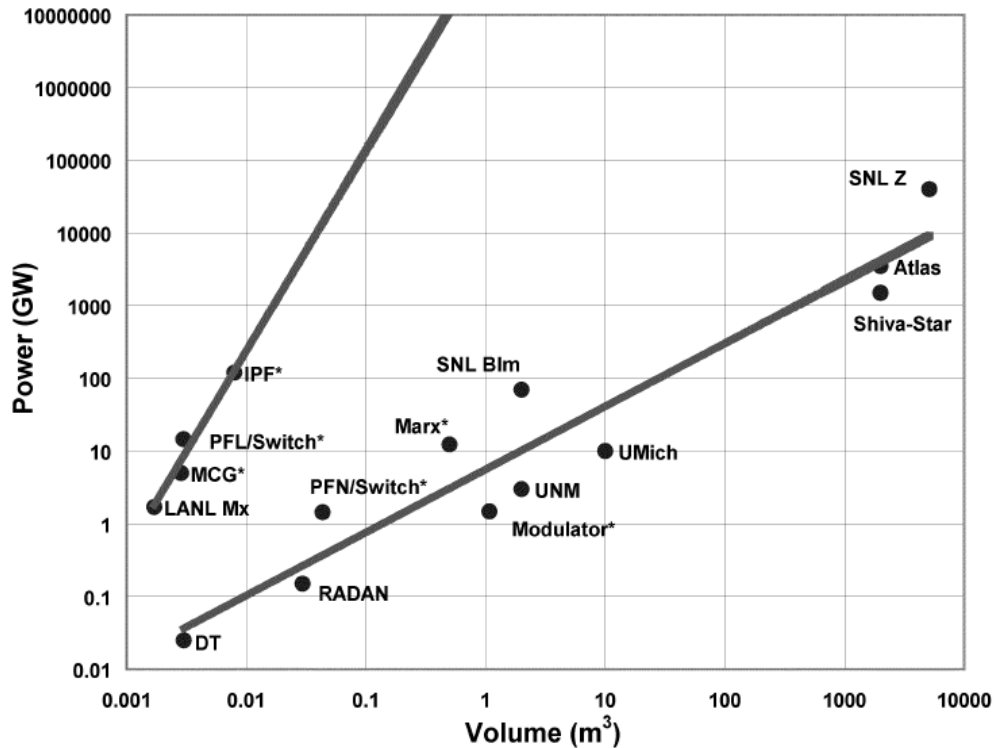
Figure 4 Analogy for mouse-to-elephant curve for pulsed power systems[2]

Reducing volumes of the system components and creating compact pulsed power systems requires increased power density of pulsed power systems. The fundamental limitations of the power density are maximum energy density of the energy storage units and the compactness of the switching components. Systems that can combine more

4

functions (such as storage of energy, scaling and shaping of the pulse) in a single volume are one of the most important motivations for today's pulsed power research [4]. Increased number of publications on compact/ultracompact pulsed power research is concentrated on different aspects of pulsed power systems. Compact capacitive storage units with high dielectric materials and compact closing switch units using both solid-state and gas-phase switches are reported [4-8].

Pseudosparks have been attracting attention as high hold-off voltage, high-current, fast risetime gas phase closing switches with moderate house-keeping requirements which are suitable for mobile platforms.

1.3   Motivation of Research

Need for the compact pulsed power systems, for both military and civilian applications, has increased the research on this subject in recent years. Key research subject for compact systems are dielectric media with better capacitive storage capabilities and high-power closing switches with less house-keeping requirements.

Among plasma switches, house-keeping requirements are reduced for pseudosparks compared to thyratrons since they do not require external heating with their self-heated cathodes. However, pseudosparks can be bulky due to the triggering mechanisms that require additional space for good electrical isolation from main part of the switch.

The primary objective of this work is to develop a triggering mechanism for pseudospark switches that is easy-to-construct, compact, and has a scope for future improvement depending on the requirements of the specific applications.

CHAPTER 2

BACKGROUND

2.1   Plasmas

Name "plasma" was first used by Irvine Langmuir for a neutral volume of charged particles in 1927 [9]. Plasma can be created by applying a potential difference between two electrodes in a gaseous medium. Electric field generated between these two electrodes- anode and cathode- causes ionization of neutral gas particles and creates a conducting path. This phenomenon is called breakdown.
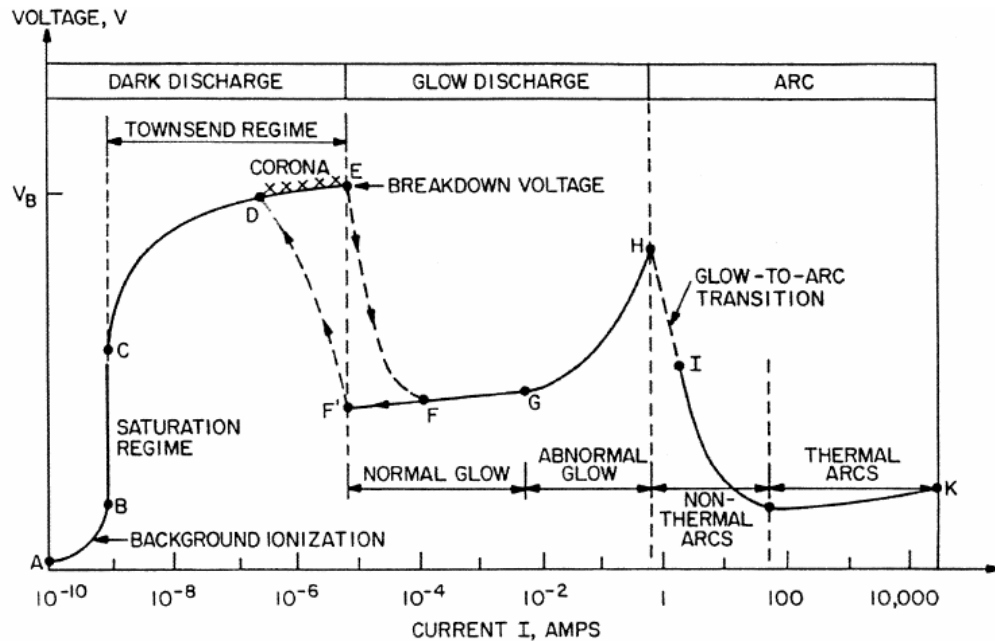
Figure 5 DC Gas Discharge V-I characteristics [10]

Electric field lines between the anode and the cathode depend on the geometry of the electrodes. The simplest configuration, where the electric field is almost uniform, is two plane electrodes with a small gap in between compared to the size of electrodes.

Figure 5 shows voltage-current characteristics of a DC low pressure electrical discharge with plane electrodes [10]. Dark discharge region is where discharge formation begins, however the discharge does not contain enough energized particles to lead to breakdown formation. This discharge is dark because there are no energy level transitions of electrons causing visible light emission. During background ionization regime of the dark discharge, individual ions and electrons created by cosmic rays and other forms of natural ionizing radiation are swept out by increasing voltage; during saturation regime, all the background ionized charged particles are removed and moreover electrons do not have enough energy to cause ionization. Townsend regime is where ionization caused by electric field starts, and the current increases exponentially with the increasing voltage. Between Townsend regime and the breakdown, corona discharges may occur as a result of local electric field concentrations on the electrode surfaces around sharp edges. Corona discharges can be visible or dark depending on the level of current supplied.

Glow discharge region is one of the main interests of this research. This region starts with the breakdown and ends with the arc formation. Glow discharge will be explained in detail in the next section.

Processes leading to the breakdown and glow discharge formation can be classified into two groups: (a) Gas processes in which ionization by electron and ion collisions is effective; (b) cathode processes in which electrons are liberated from the

cathode. Cathode processes are also called secondary processes where electron emission is effective. Experimental results in the literature indicate that the cathode material affects the breakdown phenomenon and play a major role in breakdown formation. Secondary processes can be caused by different types of energy radiations like photoelectric emission where light energy contributes to electron release, thermionic emission where thermal energy is main cause of electron emission or field emission where emission due to electric field occurs [11].

Arc discharges are intense, highly luminous, and high current density discharges. High current densities up to kiloamperes per square centimeter are easily achieved by arc discharges; however their concentrated nature causes high erosion rates of the electrodes.

2.1.1 Glow Discharge

The glow discharge is a luminous low pressure discharge which has widespread industrial applications like analytical chemistry, micro-electronics fabrication, lasers, and lamps [12]. For the electrical discharge structure mentioned in previous section; current increases exponentially with applied voltage up to the breakdown voltage. At the breakdown voltage, if the current supplied through the voltage source is sufficient, the gas will breakdown leading to the glow discharge regime. The glow discharge is a diffuse discharge unlike the arc discharge. In Figure 6, an ideal sketch showing the regions of the normal glow discharge is presented [10].
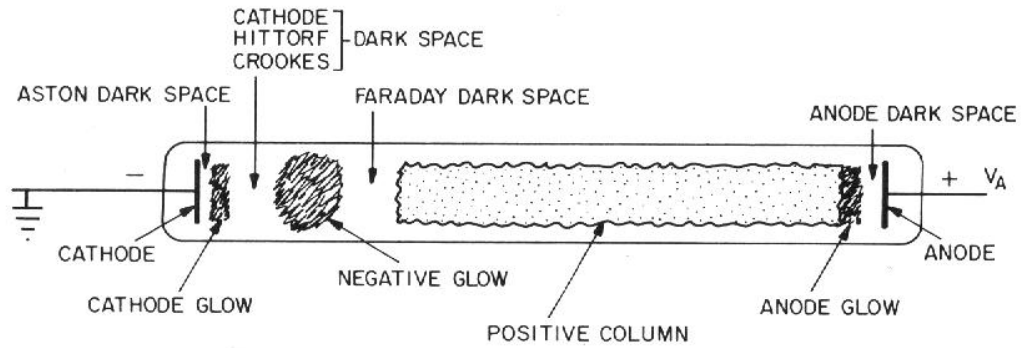
Figure 6 Regions of Normal Glow Discharge [10]

<u>Cathode</u>: Electrically conducting metal whose secondary electron emission coefficient is very important for the discharge formation.

<u>Aston Dark Space</u>: Immediately to the right of cathode, Aston dark space is a thin dark region which contains slow electrons that are too low in energy to excite the gas.

<u>Cathode Glow</u>: Bright region close to the cathode with high ion number density. This region may cling to cathode and block Aston dark space.

<u>Cathode (Crookes) Dark Space</u>: Dark region to the right of cathode glow with high ion density and positive space charge.

<u>Cathode region</u>: Most of the voltage drop across the discharge appears between cathode and the right of the cathode dark space. This region is called cathode region and the voltage drop at this region is referred as cathode fall. Most of the power dissipation occurs in this region. Length of this region is adjusted so that minimum power dissipation can be achieved.

<u>Negative glow</u>: The brightest region with intense excitation of atoms. Electrons accelerated in the cathode region produce light emitting processes. This region is usually longer than the cathode glow.

9

Faraday Dark Space: Electron number density decreases in this region. Net space charge is very low and electric field is small.

Positive Column: This region is quasi-neutral. As the length of the discharge tube is increased at constant pressure, length of cathode region remains constant and the positive column lengthens. Positive column is a long, uniform glow.

Anode Glow: Bright region close to anode that is not always present.

Anode Dark Space: Dark region next to anode with high negative space charge.

During the normal glow discharge operation both the voltage across the electrodes and the current density through the plasma remain almost constant while the current delivered by the supply increases. This regime continues until the plasma covers the entire cathode surface in order to deliver total current at constant current density. After this point both the voltage and the current density increase significantly leading to the abnormal glow discharge. At the end of the abnormal glow regime, the electrodes become sufficiently hot and the cathode emits electrons thermionically. If power source can supply sufficient current, glow-to-arc transition occurs at this point.

Glow discharge is a self-sustaining discharge with a "cold cathode." This means the electron emission is due to secondary processes, mostly because of ion bombardment of the cathode, rather than the thermionic emission [13].

2.1.2 Hollow Cathode Discharge

When a single plane cathode is replaced by a cathode with some hollow geometry, in a specific range of operating conditions, negative glow is found to be inside the hollow structure of the cathode. This effect is called the hollow cathode effect.

The hollow cathode effect is mainly caused by so-called pendulum electrons [14]. Electrons emitted from the cathode surface are found to make oscillatory motion between opposite surfaces of the hollow cathode. These reflected electrons referred as pendulum electrons undergo many ionizing collisions leading to significantly higher electron emission rates compared to parallel plate configurations. Cathode fall can be significantly thinner in hollow cathode geometries leading to increased ion velocities and increased secondary electron emission rates. Thus, hollow structure increases the probability of multiple processes and collisions for all particles creating high current density plasma inside the hollow cathode.

The hollow cathode discharge range in literature for rare gases is, in general, given as 1 torr-cm<pd<10 torr-cm where p is pressure and d is the diameter of hollow cavity [15]. Hollow electrode structures have been used for their intense electron emission properties for a long time in many applications such as spectral lamps, gas lasers, electron beam generators and high current closing switches [16].

2.1.3 Paschen Law

Paschen's law is a well known plasma physics law stating that the amount of potential difference required for a gas to breakdown is a function of pressure and gap distance product (*pd*).

$$V_{breakdown} = f(pd)$$

It was first stated by F. Paschen in his paper at 1889 [17]. Figure 7 shows a typical Paschen curve for Helium and Nitrogen gases [18]. "Paschen minimum" refers to the *pd* product where breakdown voltage is minimum.

If there exists different lengths of discharge paths between anode and cathode, Paschen minimum can occur at long-paths for low-pressures and short-paths for high pressures. The shape of Paschen curve indicates two different *pd* product values for the same breakdown voltage, one at the right-hand side, one at the left-hand side of Paschen minimum. High power plasma switches aiming to hold-off very high voltages are developed at both sides of Paschen curve, indicating either high or low pressure range operation. Thyratrons and pseudosparks operate at the left-hand side of the Paschen curve.
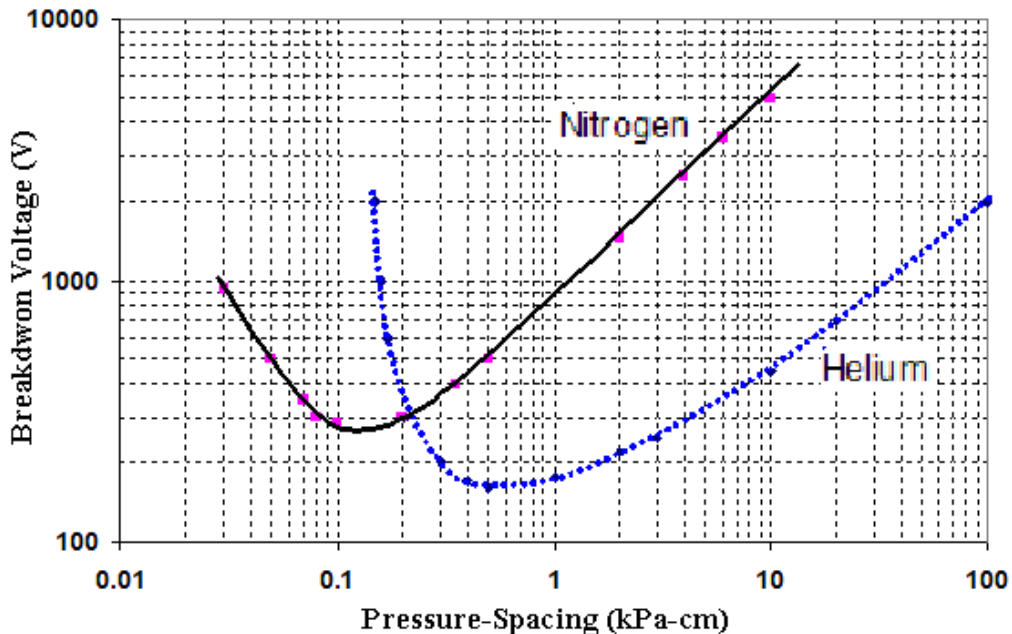
Figure 7 Paschen Curve [18]

2.2   Closing Plasma Switches

Closing switches are "open" in their natural state and are closed with an application of some sort of trigger. They can be viewed as two electrodes and a dielectric medium in between. Triggering basically increases the number of charge carriers in the dielectric medium by various mechanisms depending on the type of the switch [19]. These charge carriers act as the seed and initiate the breakdown or "closing" action.

2.2.1   Performance Related Terminology for Closing Switches [19]

Voltage Stand-off/Hold-off: Voltage where self breakdown occurs.

Peak Current: The maximum current for which switch operation is healthy.

Delay: Amount of time between the application of trigger and the initiation of conduction.

Jitter: Statistical variations in the exact time of the initiation of conduction with respect to the trigger signal.

Repetition Rate: The rate at which the switch can be closed and opened without degradation of characteristics.

Recovery Time: Time for switch to go to its initial state after opening trigger is applied. This parameter is critical in determining repetitive operation capability of the switch.

Forward Drop: Voltage across the terminals of the switch when it is at closed state. This parameter determines the power consumption of the switch.

Lifetime: Number of shots before degradation of switch characteristics occurs.

As mentioned in the introduction, high power switches are the most important components of the pulse forming stage of a pulsed power system. They are used to transfer large amounts of stored energy as high amplitude, short duration pulse to the load. Therefore, they must meet high voltage/current and short rise/recovery time requirements of the load. These requirements are usually voltages between several tens of kilovolts to megavolts and risetimes as short as nanoseconds up to microseconds.

Plasma switches have been used for their good transition properties and high voltage stand-off (hold-off) capabilities for decades in pulsed power systems. Closing plasma switches like gas filled spark gaps, ignitrons, vacuum gaps, thyratrons are reviewed in literature in detail [20, 21].

Solid-state switches are also finding increasing applications in pulsed power systems with their compact house-keeping requirements and long lifetimes. However, their limited hold-off voltage and peak current capabilities are still unable to handle the parameters of large pulsed power systems. Closing solid-state switches when operated within specifications have very long lifetimes, however one-time formation of an arc is catastrophic unlike plasma switches where this will only cause reduction of lifetime [2]. Table 1 summarizes some parameters for primary gas-phase closing switches like spark gaps, thyratrons and pseudosparks as well as solid-state closing switches like thyristor, IGBT and MOSFET.

Table 1 Summary of Gas-Phase and Semiconductor Switches for Pulsed Power Applications [2]

Switch	Hold-off Voltage (kV)	Peak Current (kA)	Forward Drop (V)
Spark Gap	100	10 to >1000	20
Thyratron	30	1-10	150
Pseudospark	35	5-100	200
Thyristor	1-5	1 to 50	2
IGBT	1	1	3
MOSFET	1	0.1	V_{DS}

2.3   Spark Gaps

Self breakdown spark gaps can be described as the simplest closing switches with two electrodes inserted in a gaseous medium. Upon application of required voltage, transition of the gas from a good insulator to a good conductor (open to close) is achieved [22].

In order to achieve better estimation of delay, and to be able to synchronize spark gaps in series or in parallel, several trigger mechanisms can be used. Triggered spark gaps include trigatron spark gaps that utilize a trigger electrode between anode and cathode, electron beam triggered spark gaps and laser triggered gas filled spark gaps [20].

Spark gaps can hold-off very high voltages and currents; however, arc formation can be very erosive at high currents, thus altering electrode characteristics. As a result, repeatability and lifetime are main limitations for this type of switches [2].

2.4 Thyratrons

Although first idea for thyratrons started as early as 1918's [23], hydrogen thyratrons have emerged during World War II as an input switch for power modulators for radars, and other applications. Hydrogen thyratron was developed by Germeshausen [24, 25]. Thyratrons are low-pressure plasma switches with a typical geometry as shown in Figure 8.
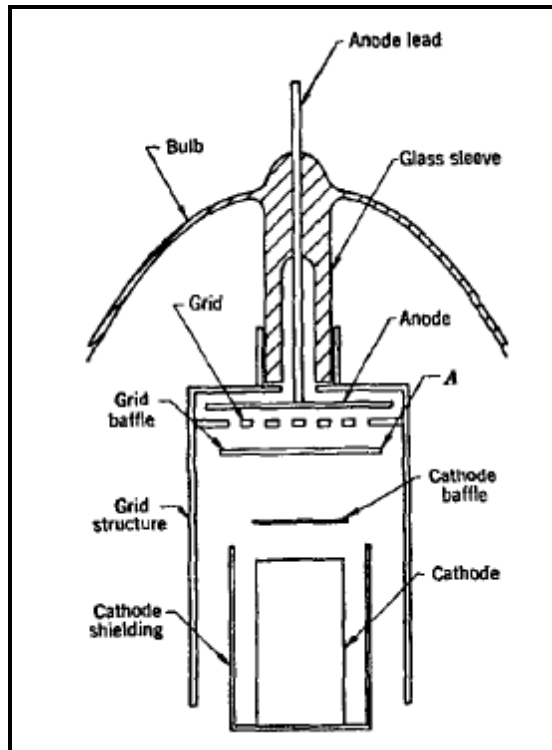
Figure 8 Geometry of a hydrogen thyratron [25]

16

Thyratrons work at the left-hand side of the Paschen curve which provides high stand-off voltages. Upon application of a positive trigger pulse to the grid, plasma formation is achieved in the grid-cathode region. This leads to closing of the switch by initiating the breakdown in grid-anode region and later connecting these two regions of plasmas. Recovery of the switch is usually achieved by starting deionization by keeping the anode voltage slightly negative. Thermionic cathodes which require external heating are used to increase peak current levels. High lifetime specifications are achieved by usage of hydrogen reservoir [26].

Early thyratrons used mercury vapor as filling gas which was replaced by hydrogen because of two big advantages. First, cathode destruction voltage for hydrogen is much higher which improves standoff voltage and lifetime parameters. Second, it has much lighter ionic mass which means much less recovery time and higher repetition rates. However, hydrogen had the disadvantage of being a chemically active atom which causes unwanted impurities in the gas. Hydrogen reservoirs containing metal hydrides which lead to reversible reaction with hydrogen as a function of temperature are the solution to this problem. These reservoirs accompany a heater to control the mentioned reversible reaction [25]. Later many improvements like ceramic envelope and multigap thyratrons lead to very high power ratings with hydrogen thyratrons.

One of the most important advantages of hydrogen thyratrons is their long lifetimes. This is due to glow discharge operation rather than arc which is the case for spark gaps. Glow discharge operation causes less erosion because of its diffused nature. Although thyratrons could not achieve high peak currents of spark gaps, they are still

17

very widely used because of their very high repetition rate capabilities and long lifetimes in many repetitive pulsed power applications.

2.5   Pseudospark Switches

Pseudosparks are low pressure plasma switches similar to thyratrons but with much higher current rise capability. Usually, higher current densities cause shorter lifetimes due to electrode erosion. However, because of special properties of the pseudospark discharge, which can prevent arcing at very high current densities, these switches have lifetimes comparable to thyratrons [27].

Pseudosparks when first discovered [28] were regarded as intense electron beam generators. Later they attracted attention as high power switches with very short current risetimes as well as high current peaks and long lifetimes. Moreover, low pressure operation providing short recovery times and therefore high repetition rates was attractive [29].

Pseudosparks have a special axisymmetric hollow cathode-hollow anode structure. At low pressures, mean free path of electrons–defined as the average distance a particle travels without making any collisions- is very long compared to the distance between the electrodes. Therefore, most of the electrons released at cathode arrive to anode without undergoing any ionizing collisions which is the reason for increased breakdown voltage at low pressures (left-hand side of Paschen curve).

However, hollow geometry of electrodes provides other possible lengths of discharge paths between anode and cathode thus decreasing breakdown voltage as a

result of hollow cathode effect [29]. Figure 9 shows electric field lines at the axis of hollow cathode- hollow anode geometry causing breakdown voltage drop at this region.
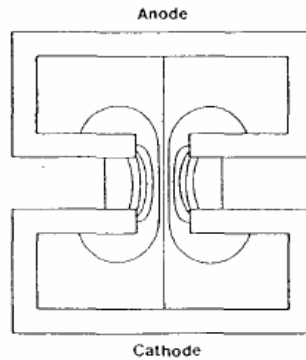
Figure 9 Electric Field Lines on the axis of a typical pseudospark geometry [30]

2.5.1 Pseudospark Discharge

Because of its hollow electrode structure, pseudospark discharge does not obey well-known Paschen curve. This new type of discharge is defined at the left-hand side of Paschen minimum [31].

Temporal development of the pseudospark discharge is well established in the literature. It involves two main phases, hollow cathode phase and high current superemissive cathode phase [32-34].

Hollow cathode phase is responsible for rapid current rise of the discharge due to the hollow cathode effect. During this phase, discharge is homogenous at the axis of the structure with a radial size equal to the bore-hole radius.

Couple of tens of nanoseconds later superemissive cathode phase starts by a change in electron emission mechanism to field enhanced thermionic electron emission. This provides a self-heated cathode process without any external heating. During this

19

phase discharge expands radially between the cathode-anode gap. High peak currents are due to this phase of pseudospark discharges [32, 34].

2.5.2 Triggering Mechanisms

Triggering is provided by introducing charge carriers to the most sensitive regions of the pseudospark which are the cathode hole and cathode backspace. Triggering by means of surface discharge, pulsed low-current glow discharge, and optical triggering are the most widely used methods [31, 35].

Pulsed Low-Current Glow Discharge Triggering: An example for this type of trigger is shown in Figure 10. Trigger module and main switch are separated by a cylindrical cage forming a hollow cathode. Pulsed hollow cathode discharge is generated inside the trigger module by applying a negative pulse to the trigger electrode. This low-current discharge initiates the breakdown in the main switch by penetrating through small holes on the cage. A blocking potential is used to accelerate the propagation of the plasma to the main switch when set to zero volts, as well as recombination of the ions and electrons when set to a positive voltage [37].
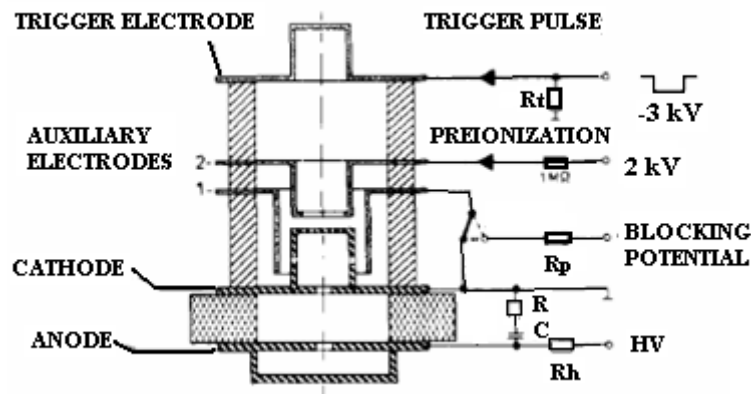

Figure 10 Pulsed Low-current Glow Discharge Triggered Pseudospark [37]

Surface Discharge Triggering: Surface discharge triggering is based on electron emission from an insulator surface. Figure 11 shows an example geometry for the surface discharge triggering. A trigger electrode embedded between two insulator discs is inserted into the hollow cathode region of the main switch. A high voltage pulse is applied to the trigger electrode to obtain emission. Insulators are required to have low breakdown voltages and long lifetimes for good switching parameters [35, 38]. Surface discharge triggering provides high peak currents and limited repeatability, whereas glow discharge triggering is more repeatable with moderate peak currents [39].
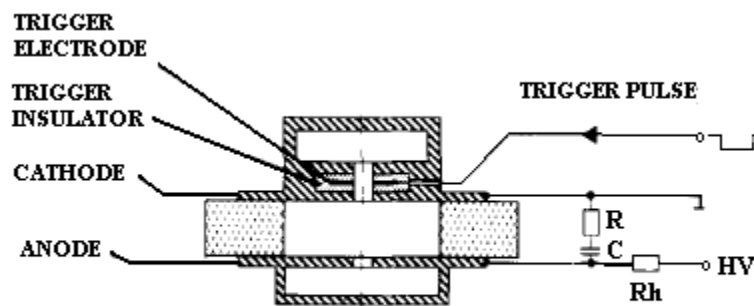
Figure 11 Surface Discharge Triggered Pseudospark Geometry [38]

Optical Triggering: Back-lighted thyratrons (BLTs) are pseudospark switches with optical triggering [16, 36] and they are triggered by photoemission using a beam of light incident on the back of the cathode in the central region of the switch. Geometry of a BLT can be seen in Figure 12. Light sources like flash lamps or lasers can be used. Optical triggering has advantages of complete electrical isolation of trigger source, simple switch structure and reliable low energy triggering. Moreover, ability to trigger

21

using fiber-optics is useful for perfect synchronization of several switches in parallel or in

series [36]. Recently, compact BLT switches are reported with 3mm aperture, currents

up to 4kA and hold-off voltages more than 20kV [7].

Figure 12 Back-lighted Thyratron [16]

Table 2 summarizes the characteristics of some commercially available sealed off

pseudospark switches. In Table 2, TDI series have trigger units based on flashover where

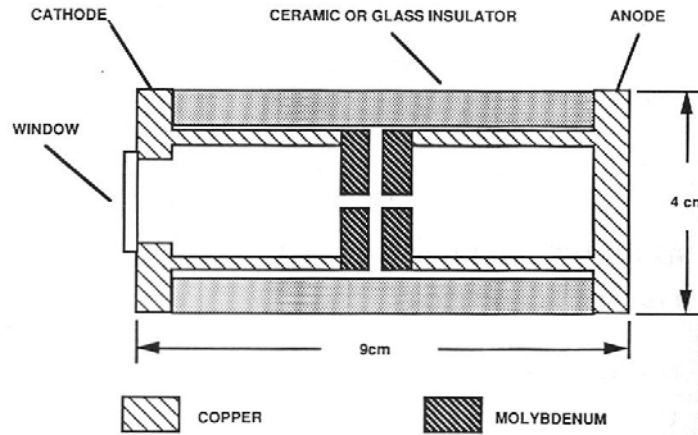as TPI series have ones based on auxiliary glow discharge [39].

Table 2 Characteristics of Sealed Pseudospark Switches [39]

SUMMARY PARAMETERS AND RATING CHARACTERISTICS OF THE SEALED-OFF SWITCHES (∅—EXTERNAL DIAMETER OF THE CERAMIC CHAMBER, H—DISTANCE BETWEEN THE CATHODE AND THE ANODE FLANGES)

Switch type	Anode voltage kV	Peak anode current kA	Average current A	Dimensions $\emptyset \times H$ mm	Total charge transfer (min) C	Pulse repetition rate kHz
TDI1-50k/16	5 ÷ 16	50	0.15	50 × 52	10^5	0.1
TDI1-50k/25	5 ÷ 25	50	0.25	98 × 80	2×10^5	0.05
TDI1-50k/50	5 ÷ 50	50	0.25	98 × 88	2×10^5	0.05
TDI1-150k/25	5 ÷ 25	150	0.5	118 × 50	5×10^5	0.05
TPI1-0.2k/12	1 ÷ 12	0.2	0.03	25 × 22	10^6	2.5
TPI1-1k/20*	1 ÷ 20	0.2	0.05	25 × 47	10^6	2.0
TPI3-10k/25*	1 ÷ 25	10	0.2	64 × 75	10^6	1.0
TPI1-10k/25	1 ÷ 25	10	0.5	98 × 95	10^6	2.0
TPI1-10k/50*	1 ÷ 50	10	0.3	98 × 101	10^6	2.0

22

CHAPTER 3

EXPERIMENTAL SETUP AND PROCEDURE

3.1   Research Objective

As stated earlier, the primary objective of this work is to develop a triggering mechanism for pseudospark switches that is easy-to-construct, compact and has a scope for future improvement depending on the requirements of the specific applications.

In order to reach the final objective stated above, series of experiments with four different electrode geometries starting with the observation of a normal glow discharge in a parallel plane configuration are conducted.   After obtaining voltage-current characteristics of the parallel plane configuration, same types of measurements are performed for plane anode-hollow cathode configuration.   For the hollow cathode scheme, the cathode is modified later on, in order to obtain improved current characteristics.   To finalize analysis of glow-type discharges, hollow anode-hollow cathode structure is used to obtain a self-sustaining pulsed hollow cathode discharge.

For the final setup, the hold-off voltage and delay measurements are conducted. Measurement methods for these important parameters are also described in the following sections.

3.2   Electrode Designs

DC glow and hollow cathode discharge experiments are conducted using three different copper electrode configurations. First configuration is a pair of parallel plane electrodes (Figure 13), second one is a plane anode-hollow cathode configuration (Figure 14) and the third one is the same configuration as second one except the holes at cathode's back surface (Figure 15). For all the configurations, the cathode is grounded and the anode is at positive potential.

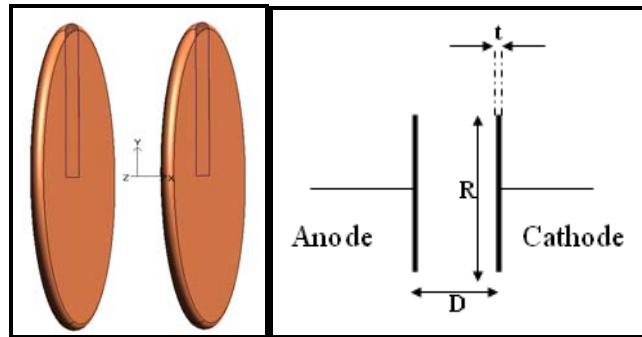### 3.2.1   Parallel Plane Anode-Plane Cathode

Figure 13 Parallel Plate Anode-Parallel Cathode

Figure 13 shows the three dimensional geometry together with its cross-section of the parallel plane electrode system. Diameter of the copper discs is R=2.2 cm; distance between the electrodes is D=0.9 cm and the thickness of the discs is t=1 mm.

3.2.2 Plane Anode- Hollow Cathode
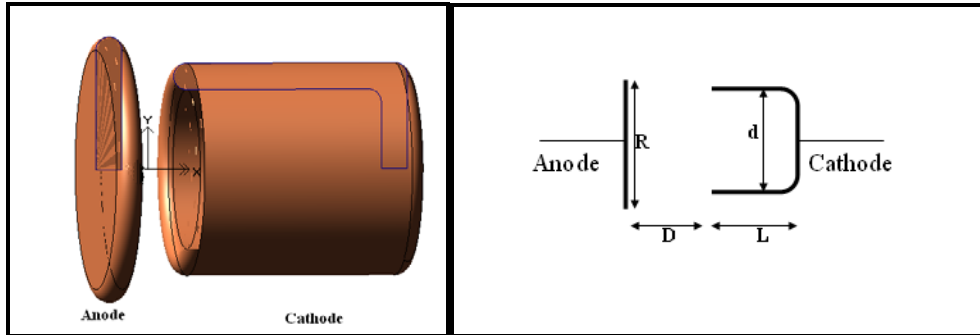
Figure 14 Plane Anode-Hollow Cathode

Plane anode-hollow cathode experiments are conducted to observe the hollow cathode effect. Plane cathode is replaced with a cylindrical hollow cathode. Dimension of the plane electrode is kept the same. The inner diameter of the cylindrical cathode is d=1.6 cm and the length of the cavity is L=1.4 cm.

3.2.3 Hollow Cathode with Holes (HCWH)

Figure 15 Hollow cathode with holes (HCWH)

Third set of experiments are conducted using the same electrodes as the previous section with a little modification. As it is shown in Figure 15, the hollow cathode is

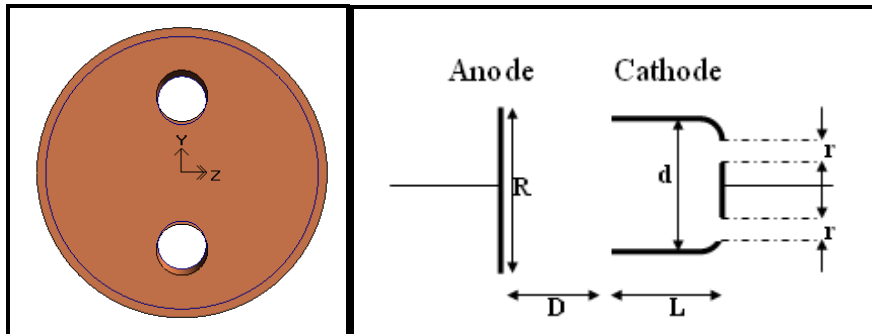modified with holes at its back surface. Diameter of the holes is r=2 mm. Back view of the cathode is also shown in Figure 15.

3.2.4 Hollow Cathode- Hollow Anode

For pseudospark switch design, hollow structures of both anode and cathode are the most common geometries. However, geometric parameters that affect breakdown formation are mostly dependent on the hollow cathode. It is reported that the most effective dimension on breakdown voltage of a pseudospark discharge in addition to the anode-cathode gap and the pressure is bore hole diameter, whereas wall thickness and the cathode cavity length are negligible under certain limits [40].

In the experiments on triggering concept, simple cylindrical hollow copper electrodes were used. Electrodes with molybdenum or tungsten-copper alloys are mostly preferred in the literature for their good erosion properties leading to good lifetime parameters, however for this initial design, lifetime considerations were not prioritized.

Based on these criteria, both anode and cathode are drilled to have a hole on the surfaces facing each other. Trigger electrode is positioned at the backspace of the cathode aligned with the bore holes of the anode and cathode. Hollow electrodes have inner diameters of 1.6 cm whereas bore holes have 2 mm diameters each. Anode-cathode gap is 3mm. Figure 16 shows the three dimensional sketch of the geometry. The electrode system is inserted in a quartz tube which also served as the holder for the electrodes. Trigger electrode is connected to a pulser supplying negative pulses up to 1kV.
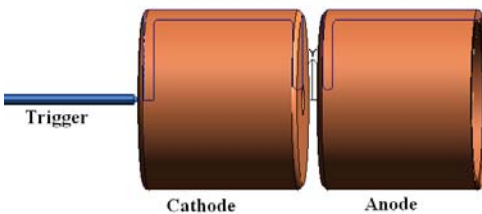
Figure 16 Hollow cathode- hollow anode electrode geometry

Pressure range of these initial set of experiments is limited to 0.8 Torr to 2.0 Torr. For pressures less than 0.8 Torr, the discharge path was not axial between the anode and cathode resulting in long-path discharges. Above 2.0 Torr, hollow cathode discharge did not occur as expected.   These initial experiments with hollow anode-hollow cathode electrode configuration are conducted using a stainless steel trigger electrode which is used as an electron emitter to start the breakdown.

Later, anode side of the glass tube holding the electrodes is sealed to prevent the long path discharges mentioned above. This lead to higher hold-off voltage levels and higher current density operation at pressures below 0.8 Torr. Furthermore, stainless steel trigger electrode is replaced by a tungsten one because of tungsten's well-known electron emission properties. A Teflon stand is used to align and hold trigger electrode for this set of experiments. Figure 17 shows the pulsed hollow cathode with stainless steel trigger electrode and Figure 18 shows the pulsed hollow cathode with tungsten electrode with sealed anode side.

27

Figure 17 Pulsed Hollow Cathode with Stainless steel Trigger Electrode

Figure 18 Pulsed Hollow Cathode With Tungsten Electrode With Sealed Anode Side
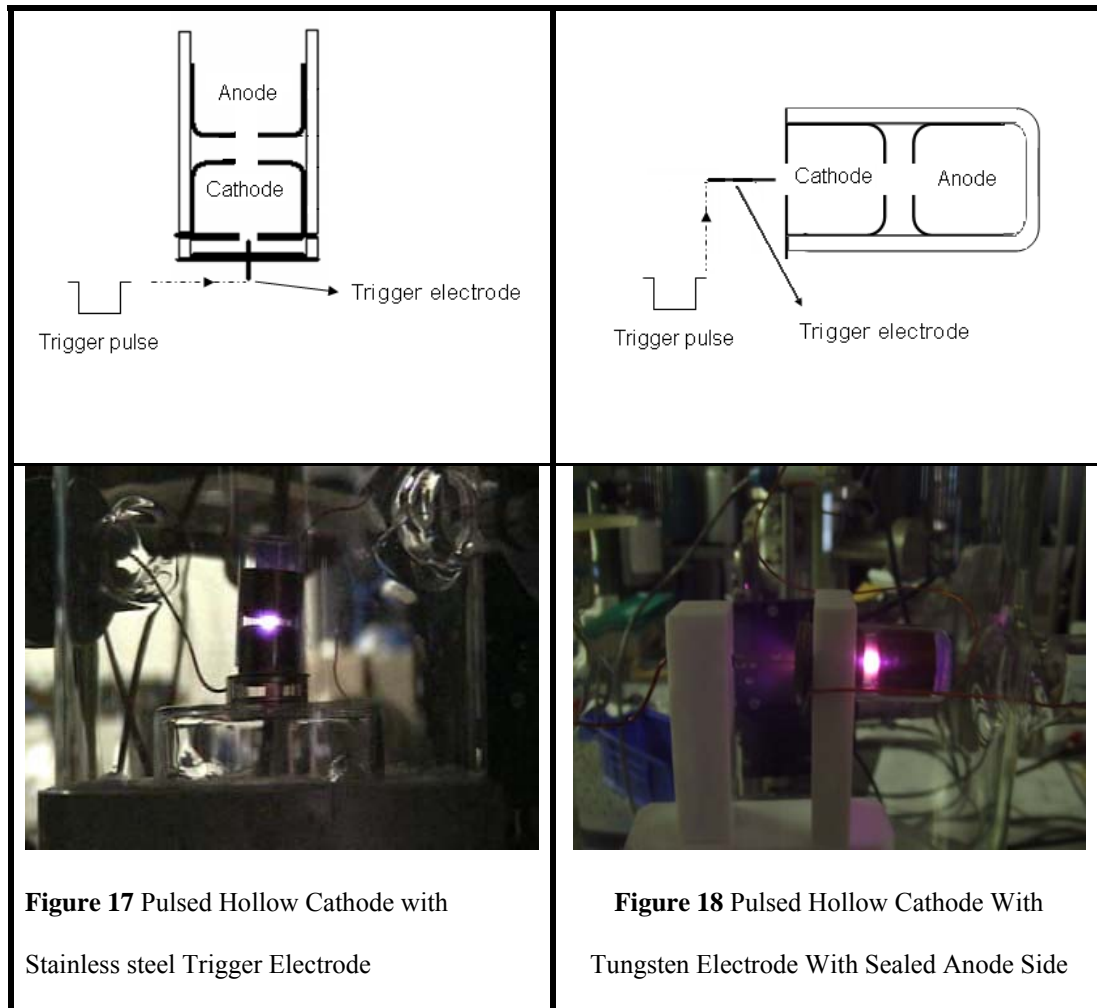
3.3   Experimental Setup

3.3.1   DC Breakdown Experiments

DC breakdown experiments include the parallel plane anode-plane cathode, plane anode-hollow cathode, and the plane anode hollow cathode with holes configurations. Experimental setup for these three configurations consists of a variable DC voltage source, a series resistance of 1 MΩ to limit the current in the circuit, and the electrodes placed in a glass vacuum chamber as seen in Figure 19.   Digital voltage and current

meters are used to measure the voltage across the chamber and the current through the circuit. Figure 19 shows the setup with parallel plane electrodes.
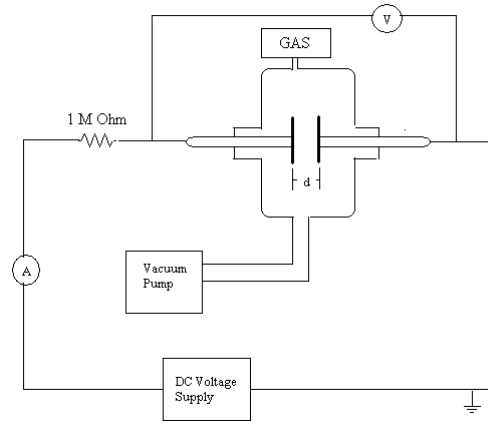

Figure 19 Experimental Setup

3.3.2   Triggered Discharge Experiments

Triggered discharge experiments include hollow cathode-hollow anode electrode configurations. The experimental setup is composed of a glass vacuum chamber and measurement instruments as in Figure 20. A variable DC voltage supply is connected to the anode and the cathode is grounded. Trigger electrode is connected to a in-house-built negative trigger pulser with maximum voltage rating of -1000 Volts. Anode voltage is measured by a Tektronix P6015 high voltage probe. A Pearson current monitor 4100 is used to measure the transient current.   Both connected to a Tektronix TDS2024 oscilloscope for data acquisition. The Pearson current probe is a 1 Volt/Ampere scaled current monitor with a sensitivity of 1%. It is used to measure different signal shapes with AC components. It does not account for DC component of the current which makes it appropriate for transient current measurements. The high voltage probe is a x1000 probe with a nanosecond response time.
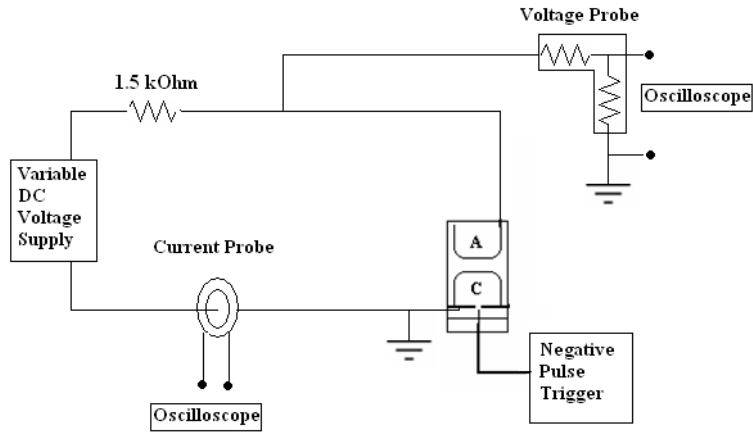
29

Figure 20 Experimental Setup

3.4 Experimental Procedure

3.4.1 DC Breakdown Experiments

In order to obtain voltage-current characteristics, voltage across the electrodes and the current through the circuit are recorded by the digital voltage and current meters as the supply voltage is increased incrementally.

For the breakdown voltage measurements across the electrodes, a Tektronix P6015 high voltage probe connected to a Tektronix 2430A oscilloscope is used. Voltage and current signals are acquired when a sudden drop in voltage across the electrodes at the breakdown is detected. Three data points are taken at each pressure and averaged. Experiments are conducted in the pressure range starting from 400 mTorr up to 2 Torr. Results are presented in the next section.

3.4.2   Triggered Discharge Experiments

This set of experiments is run in two different modes of operation: self-breakdown and triggered. Self-breakdown mode refers to breakdown initiation by varying the applied voltage across the anode and cathode until the breakdown is observed. During triggered mode of operation breakdown is initiated by a trigger voltage while the anode-cathode voltage is biased below the breakdown voltage. In this work, triggering is supplied by a negative voltage pulse applied to the trigger electrode positioned at the back of the cathode. Cathode is grounded; therefore negative trigger voltage accelerates the electrons released from the trigger electrode towards the cathode. These electrons reaching the cathode provide the energy to initiate the breakdown.

Steady state current versus bias voltage measurements

For the pulsed hollow cathode with stainless steel trigger electrode, "steady-state" current measurements are taken using a digital current meter in series with the electrodes. During the triggered operation; the bias voltage (the voltage across the anode and the cathode) is changed and corresponding steady-state currents are measured after each trigger.

Hold-off Voltage Measurements

Hold-off voltage of the hollow anode- hollow cathode geometry is measured by running the experiment in self-breakdown mode as the anode –cathode voltage is gradually increased until a breakdown occurred. Self-breakdown voltage across the electrodes is acquired when the transient current signal is detected.

Three data points for each pressure is taken and averaged. Results are presented in the next chapter.

Transient Current Measurements

The trigger voltage, voltage across the anode and the cathode, and the transient current signals are monitored through oscilloscope during triggered operation. The transient current signal is used to measure the current rise times as well as the peak current value for the experimental setup.

Delay Measurements

Trigger and anode-cathode voltage signals are monitored simultaneously and the waveforms are recorded for each shot. Arrows on Figure 21 show the delay measurement for a typical shot.
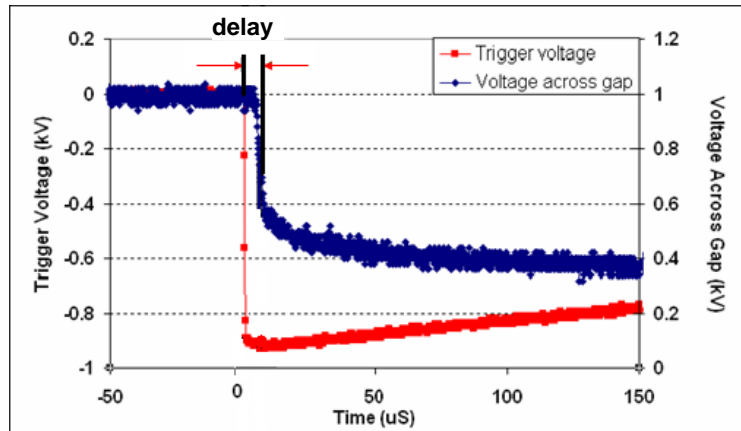

Figure 21 Delay Measurement

CHAPTER 4

EXPERIMENTAL RESULTS

4.1   Parallel Plane Anode- Plane Cathode

Regions of glow discharge were observed for parallel plane anode- plane cathode configuration. Glow appeared as a thin disc close to the cathode. This bright disc is recognized to be the positive column. Negative glow was not clearly observed since it is a very thin region for the gap distance in this setup. Dark space between the positive column and anode was clear and recognized as the anode dark space. Positive column's brightness and diameter increases as the voltage increases.

Experimental data was taken starting from the dark discharge region up to the point where glow started to cover the edges of the cathode and became an abnormal glow discharge. Data is obtained with Helium, Argon and Nitrogen as the operating gases for this set. For each gas, a certain pressure range was studied based on the stable operation of the glow discharge. Figure 22, Figure 23, and Figure 24 are the voltage-current characteristics of gases studied. The arrow on the figures indicates the breakdown initiation. The left of this arrow is the dark discharge region and right of the arrow is the normal glow discharge region.

After the voltage current measurements, breakdown voltage as a function of pressure for Nitrogen and Argon is recorded. The data is shown in Figure 25 and Figure

26. From these experiments, pressure ranges for the following experiments with the other electrode configurations are determined. Dashed curves on the Figure 25 and Figure 26 indicate the Paschen curve-like trend of the breakdown voltages.
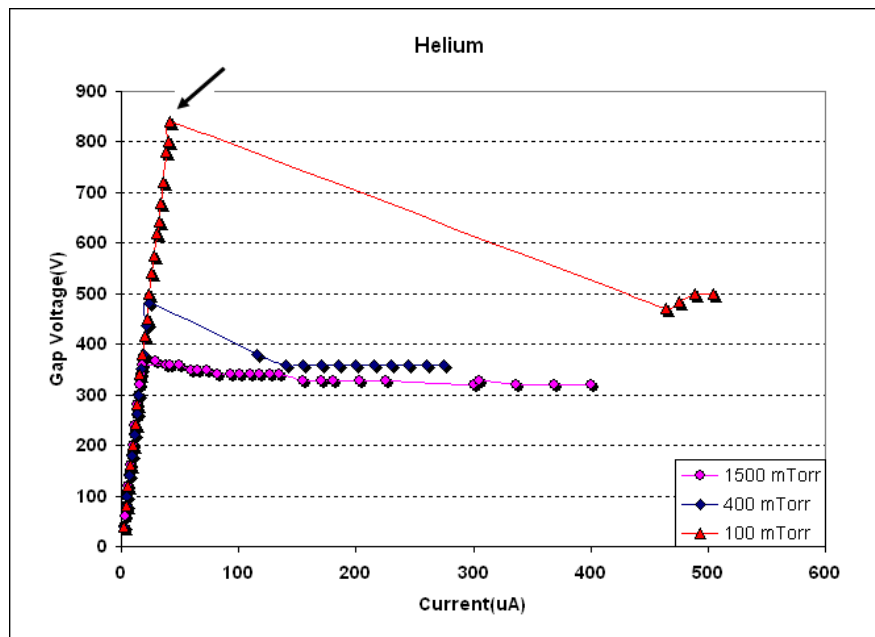
Voltage-Current Characteristics

Figure 22 Voltage current characteristics of Helium with parallel plane electrode geometry for three different pressures. The arrow shows the breakdown voltage at 100 mTorr.
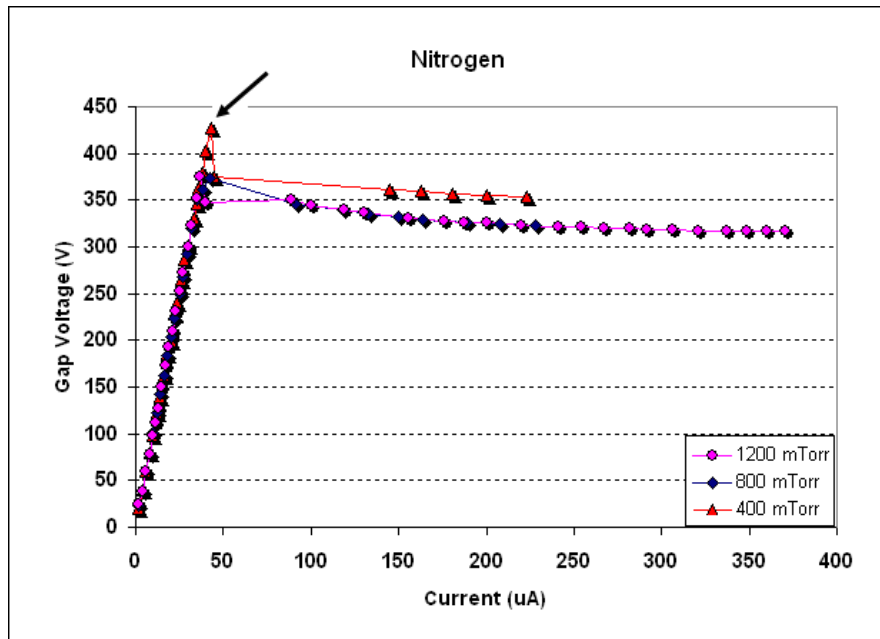
Figure 23 Voltage current characteristics of Nitrogen with parallel plane electrode geometry for three

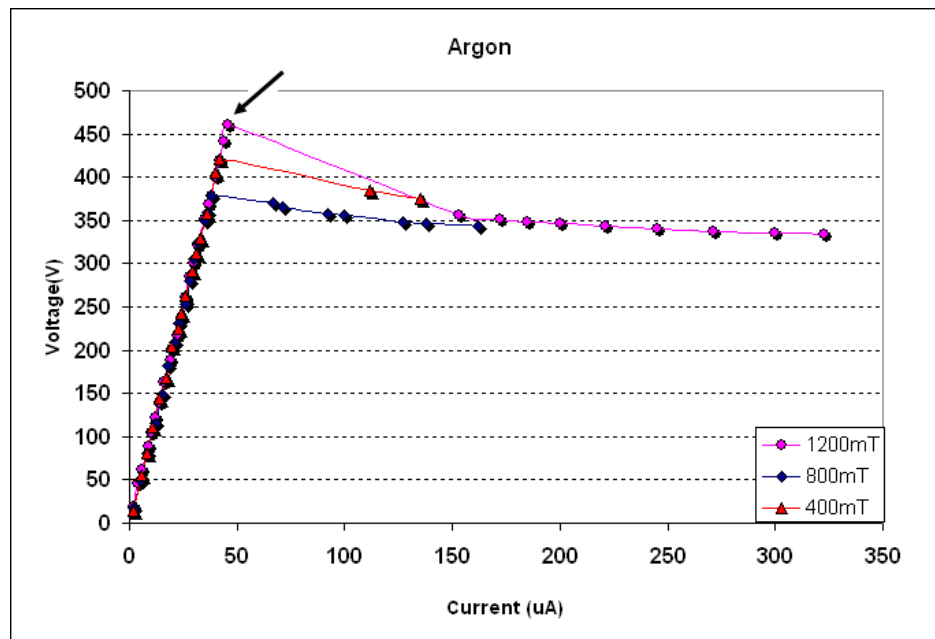different pressures. The arrow shows the breakdown voltage at 400 mTorr.

Figure 24 Voltage current characteristics of Argon with parallel plane electrode geometry for three

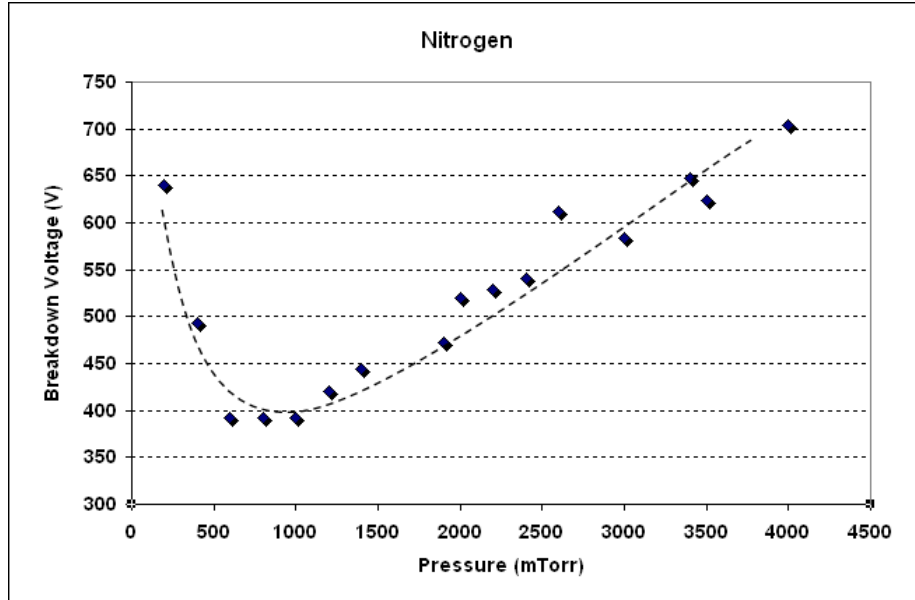different pressures. The arrow shows the breakdown voltage at 1200 mTorr.

Breakdown Voltages

Figure 25 Breakdown voltage versus pressure for parallel plane electrode geometry with Nitrogen.

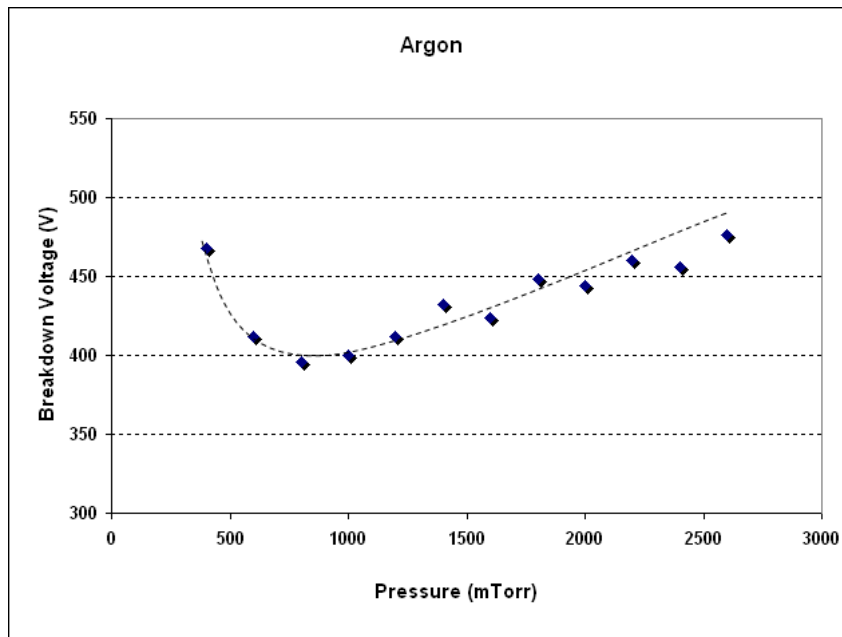Dashed line shows the Paschen curve-like trend of the data points.

Figure 26 Breakdown voltage versus pressure for parallel plane electrode geometry with Argon. Dashed

line shows the Paschen curve-like trend of the data points

4.2   Plane Anode-Hollow Cathode

Negative glow is observed inside the cathode cavity for plane anode-hollow cathode configuration.   Pressure range of operation is limited by hollow cathode discharge operation for these set of experiments.   This range is 300 to 1200 mTorr for both Nitrogen and Argon.   Outside this range, the glow is observed either outside the cathode cavity or did not develop Voltage current characteristics are shown for three pressures in this range in Figures 27 and Figure 28.   Arrows on the figures indicate the breakdown, left of the arrow is the dark discharge region and the right of the arrow is hollow cathode discharge region.

Breakdown voltage measurements are carried out for the full hollow cathode pressure range.   Figure 29 and Figure 30 show the breakdown voltage as a function of pressure for this setup.
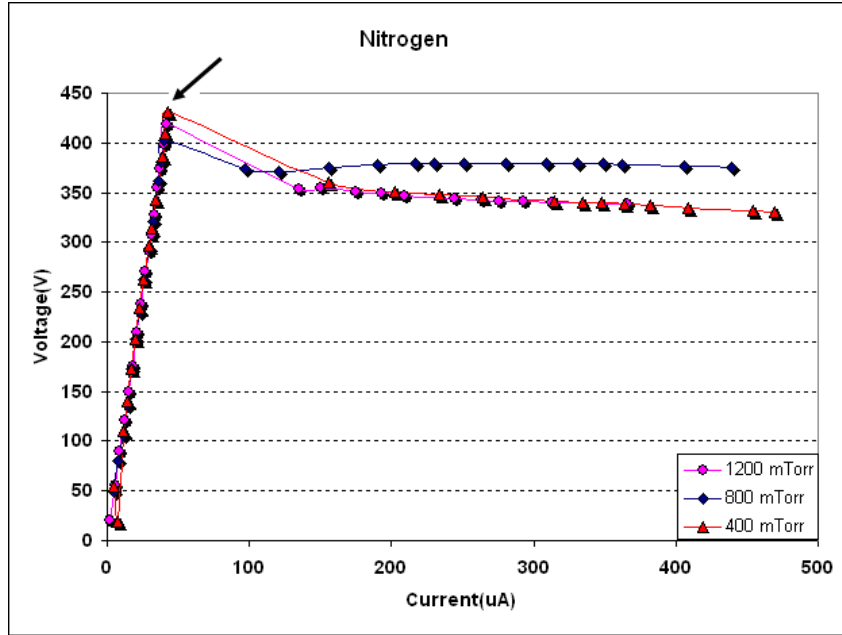
Voltage-Current Characteristics

Figure 27 Voltage current characteristics of Nitrogen with plane anode-hollow cathode electrode

geometry. The arrow shows the breakdown voltage at 400 mTorr
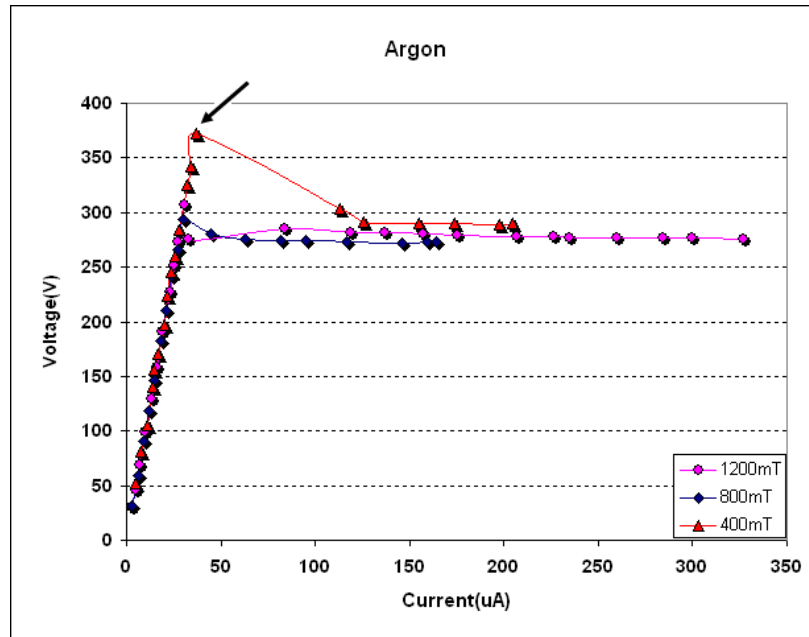

Figure 28 Voltage current characteristics of Argon with plane anode-hollow cathode electrode geometry.

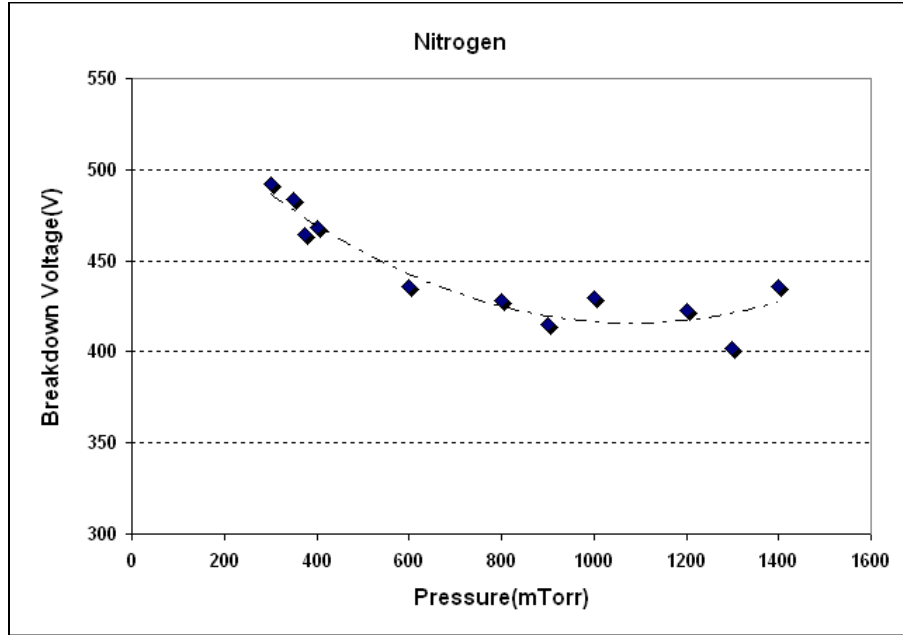The arrow shows the breakdown voltage at 400 mTorr.

Breakdown Voltage

Figure 29 Breakdown voltage versus pressure for plane anode-hollow cathode geometry with Nitrogen.

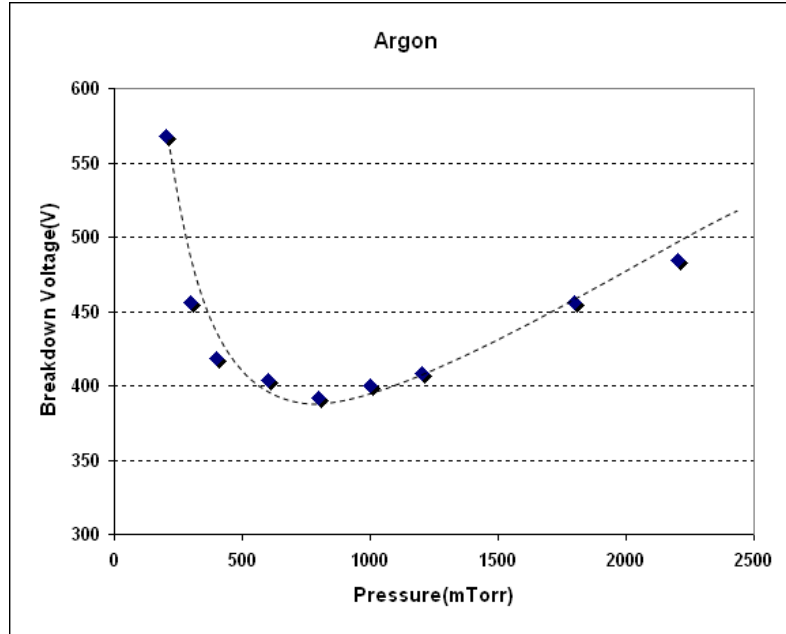Dashed line shows the trend of the data points

Figure 30 Breakdown voltage versus pressure for plane anode-hollow cathode geometry with Argon.

Dashed line shows the Paschen-like trend of the data points

4.3 Plane Anode-Hollow Cathode with Holes

Hollow cathode discharge pressure range where the negative glow was inside the cathode cavity has increased as a result of holes on the cathode back surface. This region is 400 to 2200 mTorr for Nitrogen and 400-2400 mTorr for Argon. The voltage-current characteristics of this setup are shown in Figure 31 and Figure 32. At high pressures a voltage jump is observed in voltage current characteristics with Argon as shown in Figure 33.

Breakdown voltage measurements are shown in Figures 34 and 35 where the Paschen curve-like trend is indicated with dashed lines.
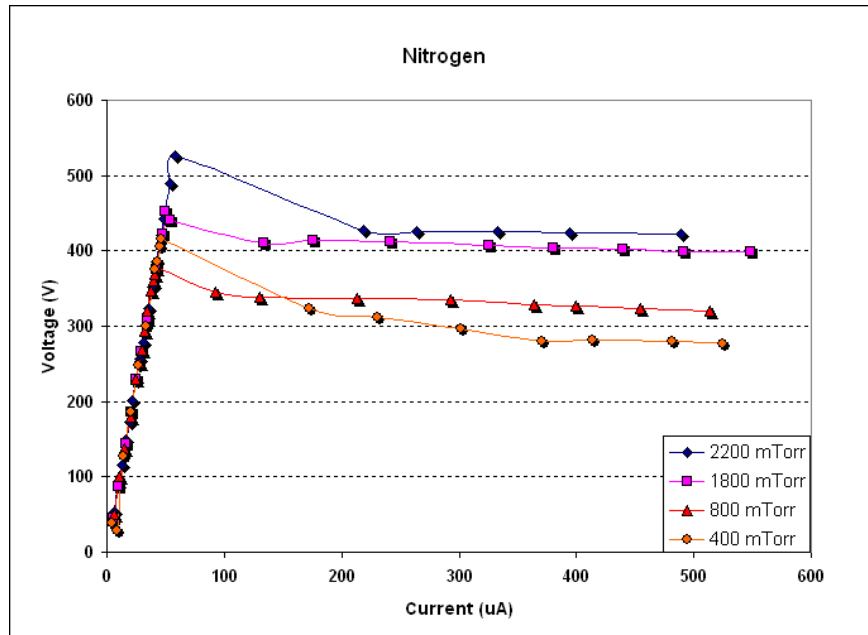
Voltage-Current Characteristics

Figure 31 Voltage current characteristics of Nitrogen with plane anode-hollow cathode with holes electrode geometry
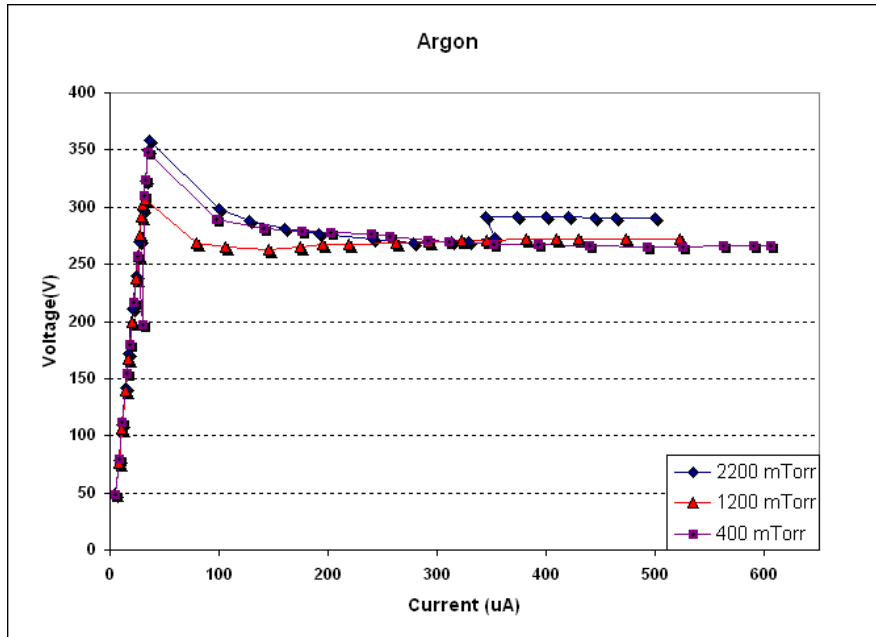
Figure 32 Voltage current characteristics of Argon with plane anode-hollow cathode with holes electrode geometry
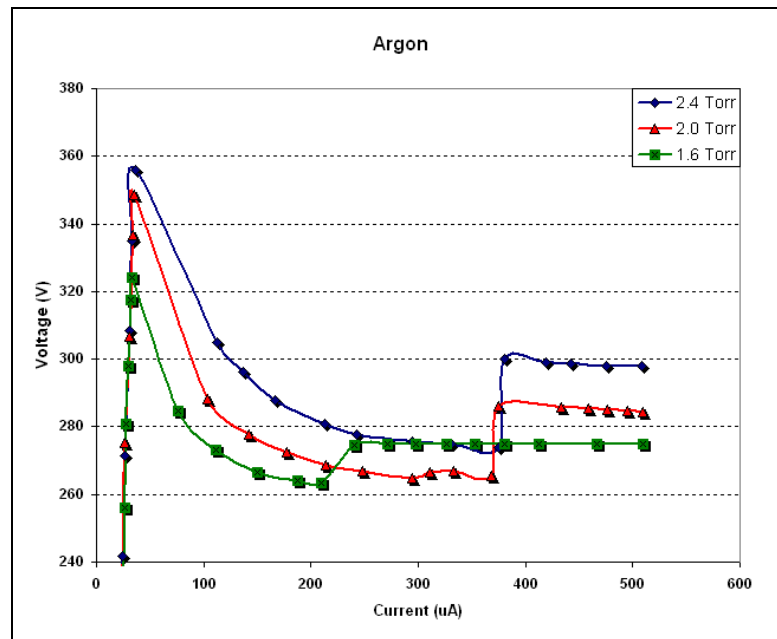
Figure 33 Voltage–current characteristics of Argon for pressures above 1.6 Torr.

Breakdown Voltage
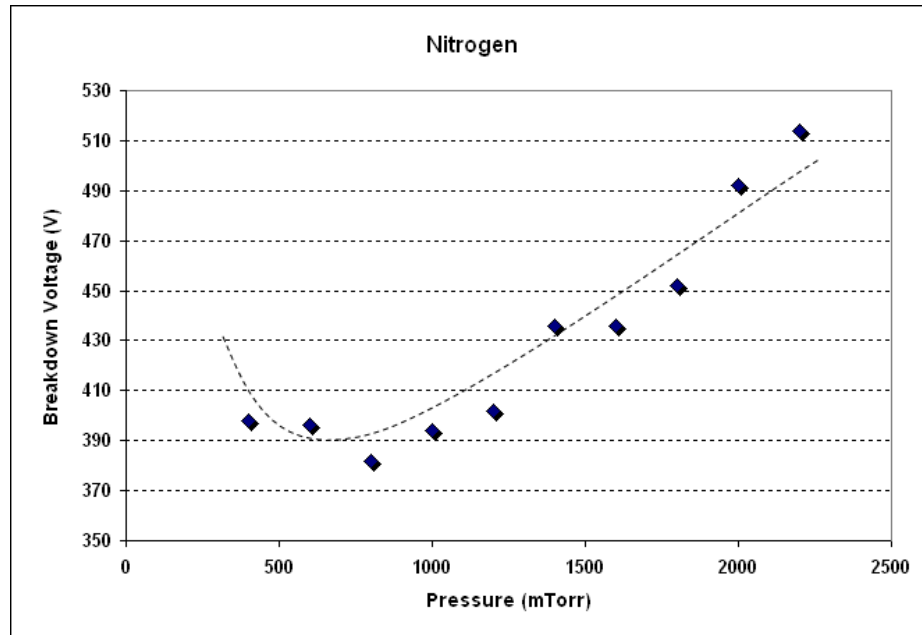
Figure 34 Breakdown voltage versus pressure for plane anode-hollow cathode with holes geometry with

Nitrogen. Dashed line shows the Paschen-like trend of the data points
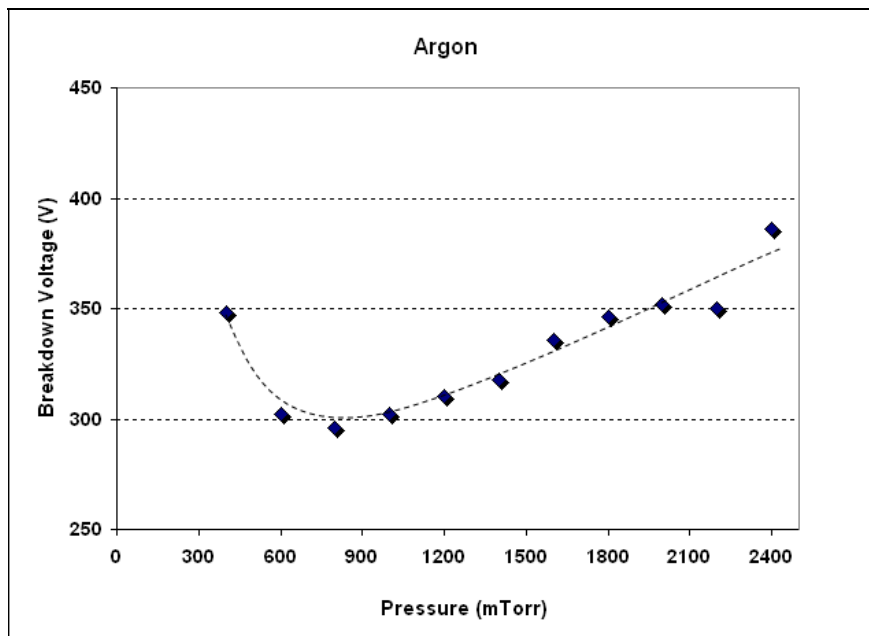
Figure 35 Breakdown voltage versus pressure for plane anode-hollow cathode with holes geometry with

Argon. Dashed line shows the Paschen-like trend of the data points

Comparison of DC Breakdown Experiments
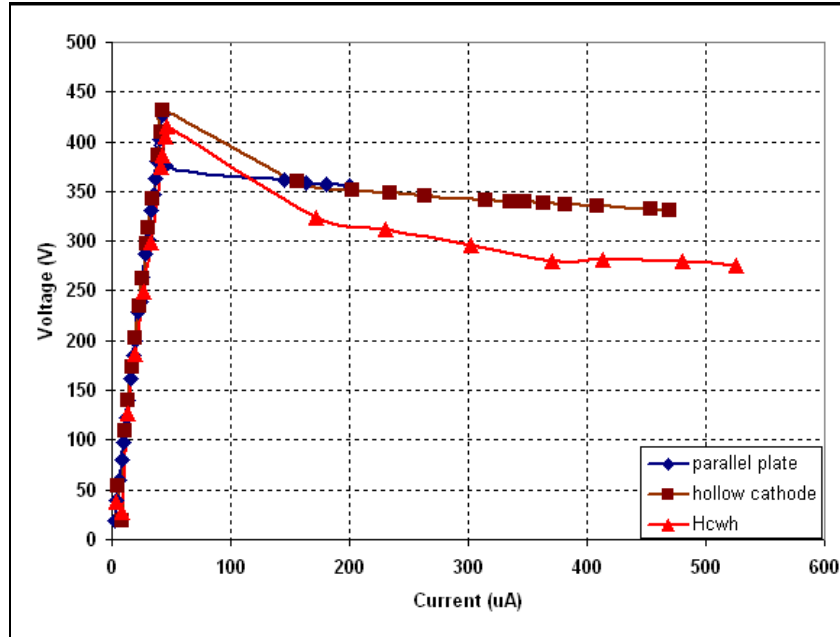
Figure 36 Voltage Current Characteristics at 400 mT with Nitrogen for different configurations

Voltage-current characteristics seen in Figure 36 shows current increase for the same voltage from parallel plane to hollow cathode configuration and from hollow cathode to hollow cathode with holes configuration. This increase is due to hollow cathode effect. For HCWH case, a second hollow cathode discharge operation region is provided as a result of holes at the cathode which increases pressure range where hollow cathode effect is observed.
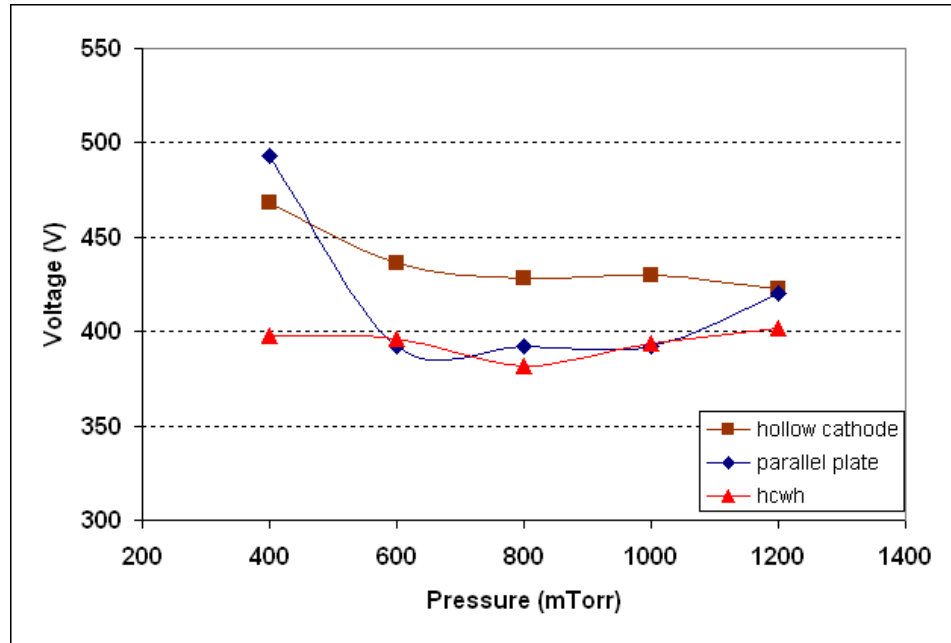
Figure 37 Breakdown Voltage versus Pressure with Nitrogen for different configurations

Breakdown voltage data is shown in Figure 37. Breakdown voltage range is significantly narrowed for hollow cathode and HCWH configurations. The effect of increased number of discharge paths as a result of hollow cathode configurations can be seen in this decrease of breakdown voltage values.

4.4 Hollow Anode- Hollow Cathode

Steady State Current versus Bias Voltage Measurements

Steady state current is the DC current of the glow after the breakdown occurs. Relation between the steady state current and bias voltage is found to be exponential. Current measurements are conducted three times for each pressure and bias voltage combination and their averages are plotted in Figure 38.
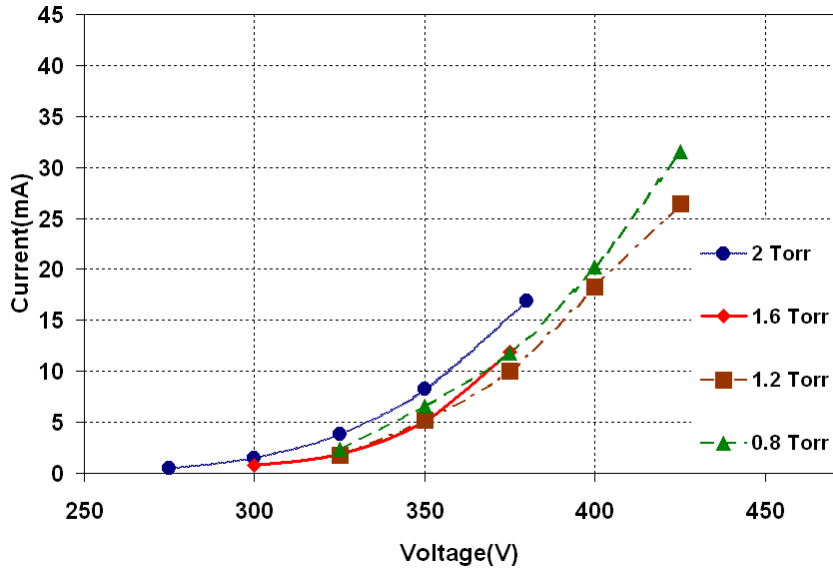
Figure 38 Steady State Current versus Bias Voltage with Nitrogen for the initial pulsed hollow cathode discharge (anode is not sealed)

Least square curve fittings in the form of $I = n_1 \times e^{\left(V_{bias}/n_2 \right)}$ are constructed where I is the steady-state current in milliamperes and V_{bias} is the bias voltage in volts. Coefficients n_1 and n_2 for each pressure are listed in Table 3. Relationship between pressure and coefficients n_1 and n_2 are shown in Figure 39.

Table 3 Coefficients n_1 and n_2 for curve fittings

Pressure(Torr)	n_1 (mA)	n_2 (V)
0.8	80 x 10^{-5}	39.84
1.2	40 x 10^{-5}	37.45
1.6	2 x 10^{-5}	27.85
2.0	6 x 10^{-5}	29.85
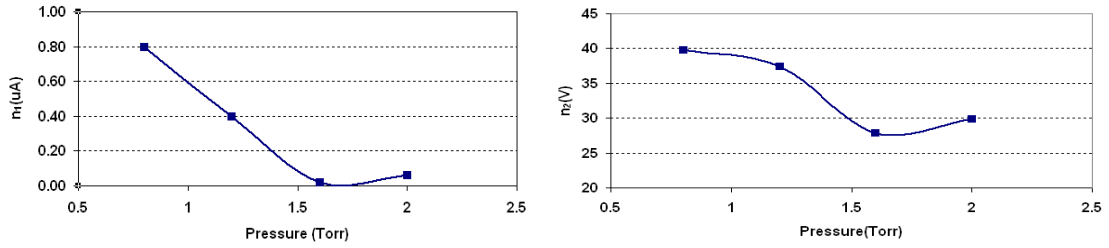
Figure 39 Relationship between coefficients n_1, n_2 and pressure

Trigger to hollow cathode discharge transition is observed on the axis of design. Hollow cathode discharge propagates through bore holes and sustains axially. In figure 40, experimental setup is seen before trigger, at the moment of trigger pulse application and after trigger is applied.
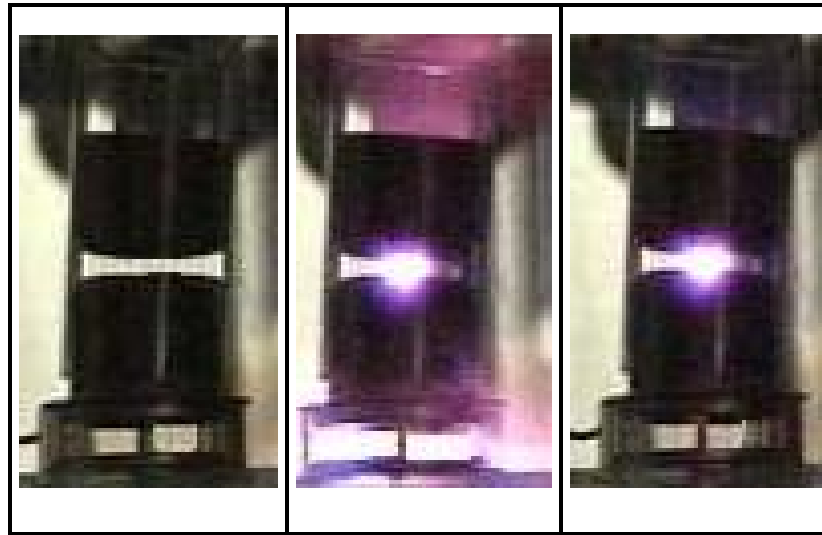
Figure 40 Temporal Development before trigger, at the moment of trigger pulse application and after trigger

Hold-off Voltage

Hold-off voltages of the hollow anode-hollow cathode electrode configuration without and with sealed quartz enclosure of the anode are measured. These experiments are run in self-breakdown mode (no trigger voltage is applied). Figure 41 shows the hold-off voltage of the hollow anode-hollow cathode electrode configuration without quartz enclosure of the anode. As seen at the figure, hold-off voltages were low. Therefore the anode side of the quartz tube is sealed for the following experiment set.
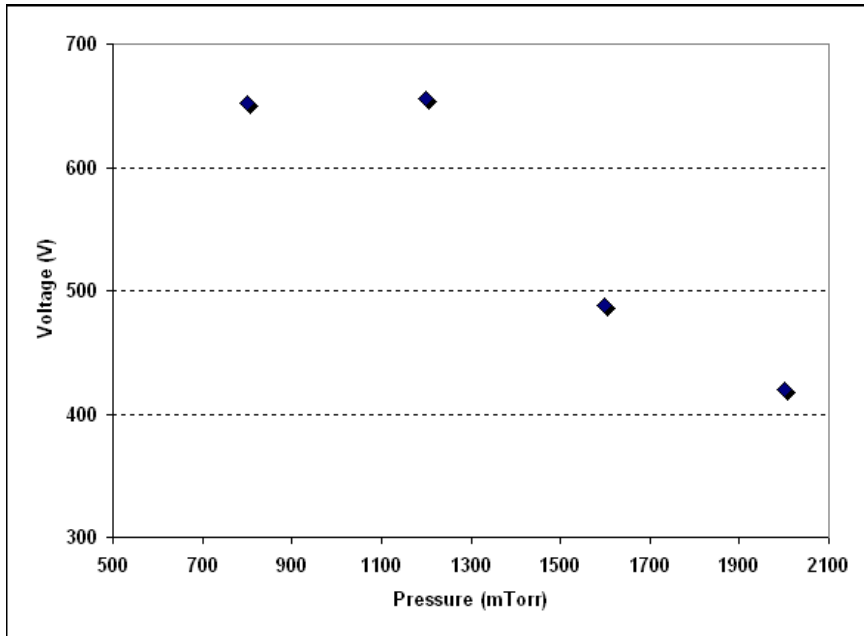
Figure 41 Hold-off voltages using Nitrogen of initial pulsed hollow cathode discharge with hollow anode-hollow cathode electrode configuration.
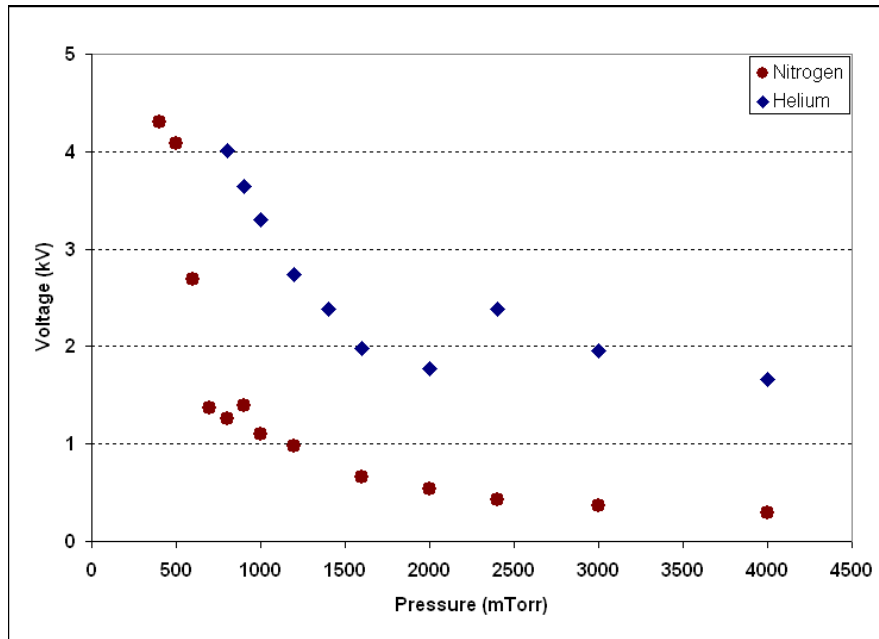
Figure 42 Hold-off voltage versus pressure with Nitrogen and Helium gases for the anode-sealed version of the pulsed hollow cathode discharge scheme with hollow anode-hollow cathode electrode configuration

Hold-off voltage measurements were carried for both Nitrogen and Helium gases for the anode sealed hollow anode-hollow cathode configuration (Figure 42). At the lower pressure border we were limited by 6kV voltage supply. For Helium lowest pressure where we have seen self-breakdown before 6kV is 800 mTorr whereas same pressure for Nitrogen is 400 mTorr. This difference between Nitrogen and Helium is expected due to difference between their Paschen minimum which can be seen in Figure 7.

Pseudospark discharge operation is at the left-hand side of Pashen curve, as mentioned in previous chapters. Since Paschen minimum of Nitrogen is lower than Helium, for the same pressure and electrode gap, helium would have a higher breakdown voltage gap at the left-hand side of the curve.

Hold-off voltages up to >4kV is observed for both gases. This parameter can be further improved easily for lower pressures.

Delay Measurements

In order to show the effect of trigger voltage on delay, delay versus trigger voltage data is recorded at 500 mTorr constant pressure with Nitrogen. As shown in Figure 43, delay decreases significantly as the trigger voltage magnitude is increased. At -900V trigger voltage, delay is a little over ten microseconds at this pressure.
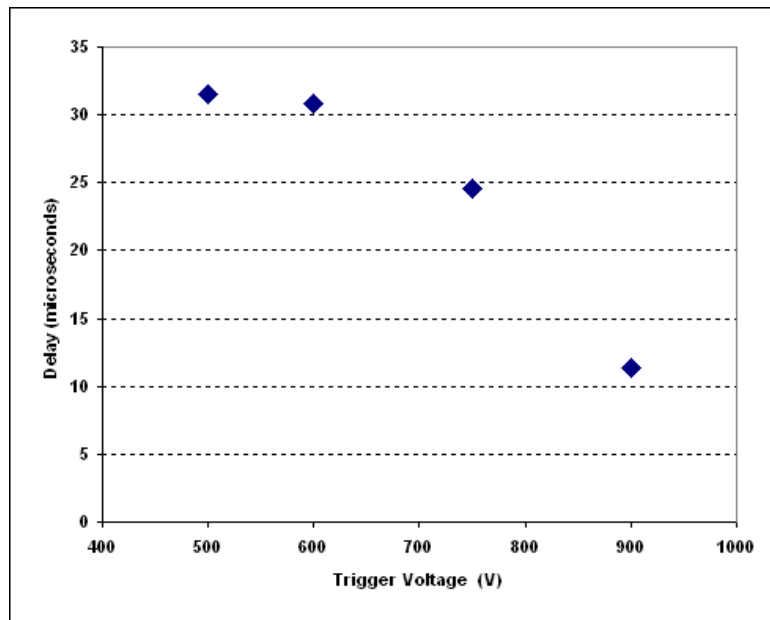
Figure 43 Delay vs Trigger Voltage at 500mT with Nitrogen

The next set of data relating pressure to delay is recorded keeping trigger voltage constant at -900V for both Nitrogen and Helium gases are shown in Figures 44 and 45. It can be clearly seen that delay is decreasing as the pressure increases for Nitrogen. This causes a trade-off between hold-off voltage and delay.

Delay measurements with Helium were not very successful because of the power supply limitations. Voltage oscillations at the output of the supply caused stability

problems to bias the anode at the desired voltage. Data for the whole pressure range were not able to be taken; Figure 46 is a summary of the data obtained. The difficulties also can be due to voltage limitation of trigger pulse we used. Trigger voltage magnitudes of 1kV can were found to be insufficient to initiate the breakdown.
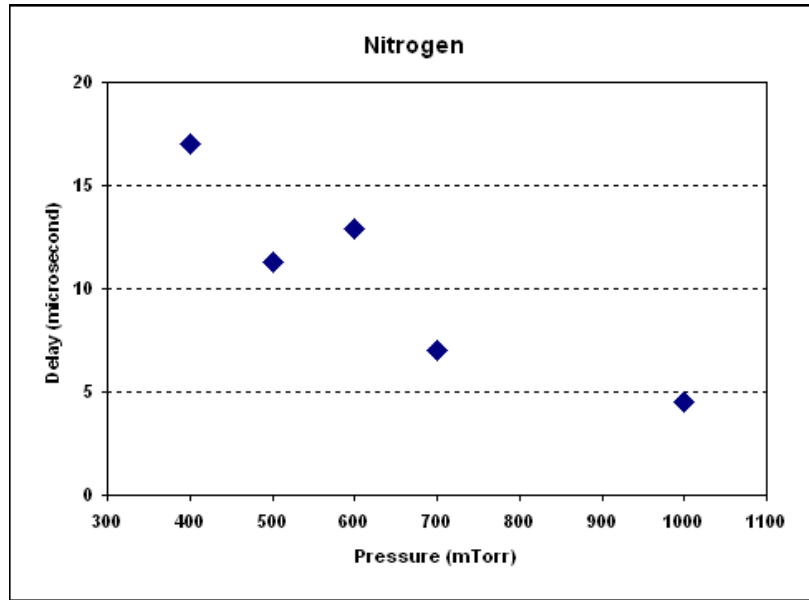
Figure 44 Delay versus Pressure for Nitrogen
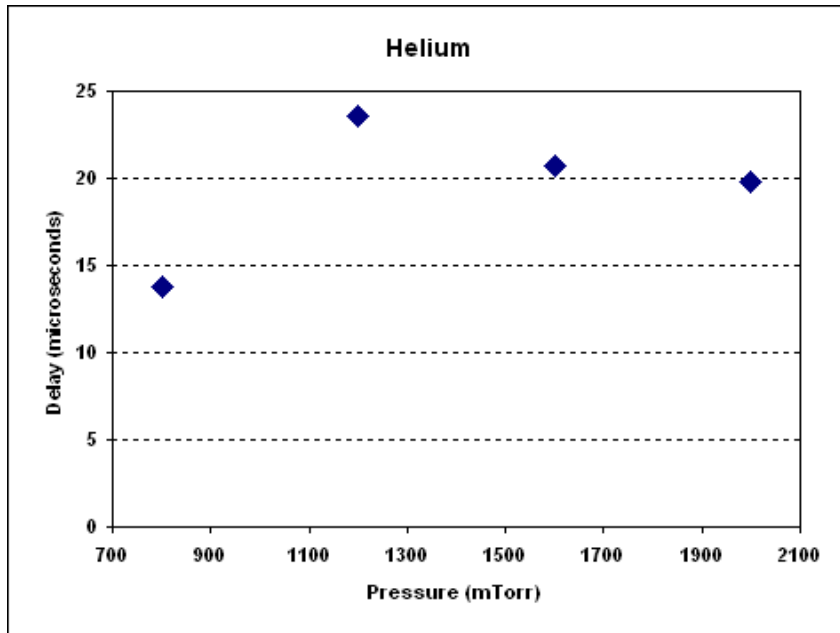
Figure 45 Delay vs Pressure for Helium

Transient Current Measurements

      Transient current measurements were carried out with limiting resistor present as shown in experimental setup section. Transient currents more than 3A corresponding to 95 A/cm^2 current densities are reached. For the measurements to determine the peak current parameter for this configuration, a limiting resistance comparable to the switch's resistance is required. These measurements were not possible with current safety regulations we have in our laboratory.

      Current rise times and voltage fall times of couple of microseconds are observed in the pressure range of our experiments.

| **Figure 46** Discharge at the trigger application instant | **Figure 47** Discharge after trigger application |
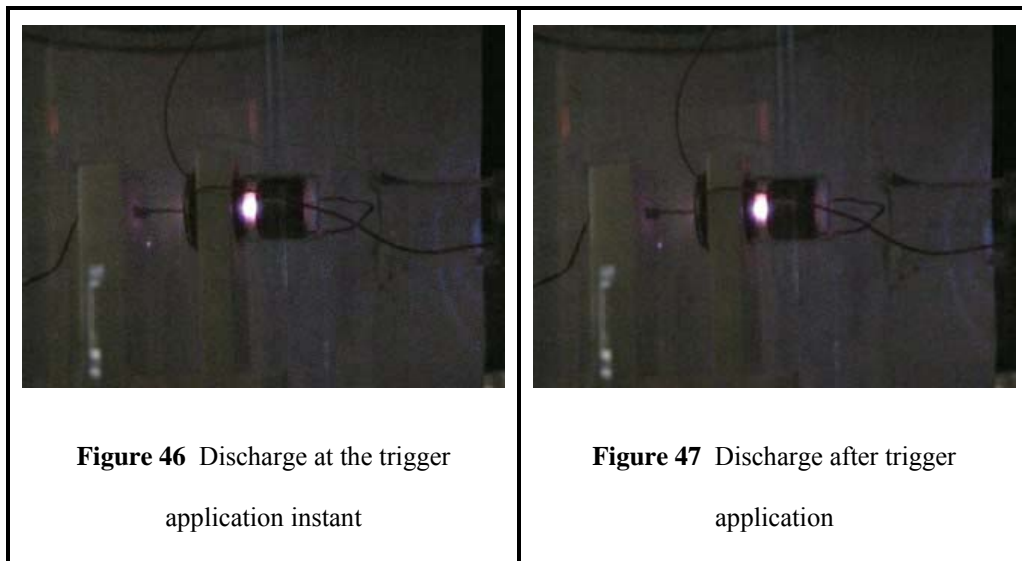
      Figures 46 and Figure 47 are snapshots from a video recorded during operation of this switch. At the trigger instant glowing around the trigger electrode can be seen.

CHAPTER 5

DISCUSSION AND SUMMARY

As today's pulsed power technologies priorities compactness as well as high hold-off voltages and high peak current densities, pseudosparks are very advantageous with their scalable symmetric geometry and high voltage/current parameters that may be catastrophic for semiconductor switches.

In this research, we conducted a series of experiments to analyze glow type discharges.   Also, a compact pulsed hollow cathode discharge configuration was designed and constructed.   This setup was further improved to reach high hold-off voltages of up to 4 kV, which is used to test an easy-to construct and simple triggering idea for pseudospark type high power switches.   Triggering using a tungsten trigger electrode as initial electron emission source was achieved and tested for fundamental parameters.

For initial discharge analysis we obtained the well-known normal glow and hollow cathode discharges.   With parallel plate electrode configuration, regions of the normal glow discharge such as positive column and anode dark space were observed. Hollow cathode discharge where negative glow is inside the cathode cavity was also observed.   Hollow cathode discharge operating pressure range was expanded with holes

drilled to the cathode's back surface. This configuration also allowed increased current densities of the discharge.

Electrically triggered pulsed hollow cathode discharge is designed and built using hollow anode- hollow cathode electrode configuration. Axisymmetric nature of this configuration is the same as pseudospark type structures. Hollow cathode discharge is tested for 0.8 to 2.0 Torr pressure range. Bias voltage versus steady-state current relation is found to be exponential by curve fitting the experimental data as follows:

$$I = n_1 \times e^{\left(V_{bias}/n_2\right)}$$

The coefficients n_1 and n_2 are found to have a similar behavior with respect to pressure with a minimum at 1.6 Torr.

Pulsed hollow cathode discharge is initiated with a negative trigger pulse application. After triggering, discharge propagates through the bore holes and sustains axially. Hollow cathode-hollow anode configuration used for pulsed hollow cathode scheme is improved to hold-off voltages as high as 4kV by sealing the anode side of the quartz tube holding the electrodes. Microsecond range delays are observed at these experiments. These parameters can be further improved with the help of higher rated, more stable power supplies. Hold-off voltage measurements can be widened by going to lower pressures which will lead to higher stand-off voltages which were limited by our voltage source at these experiments.

Using same triggering concept, closed trigger units with other electron emitting materials can be tested for improved device characteristics.

High hold-off voltages that are suitable for high-current density operation are achieved. However, current-density is limited by a series limiting current resistor. For future testing, peak current measurements can be carried out using a resistance comparable to switch resistance and higher scale current probe. Superemissive cathode phase of pseudospark discharge can be observed at these high current density operation. However, the increase in current density may cause limitations on lifetime of the electrodes. In order to improve expected lifetime of the electrodes using molybdenum or tungsten-copper can be implemented.

REFERENCES

[1]   M. Kristiansen, "PULSED POWER APPLICATIONS," in *Pulsed Power Conference, 1993. Digest of Technical Papers. Ninth IEEE International*, 1993, p. 6.

[2]   E. Schamiloglu, R. J. Barker, M. Gundersen, and A. A. Neuber, "Modern Pulsed Power: Charlie Martin and Beyond," *Proceedings of the IEEE,* vol. 92, pp. 1014-1020, 2004.

[3]   E. Schamiloglu and R. J. Barker, "Special Issue on Pulsed Power: Technology and Applications," *Proceedings of the IEEE,* vol. 92, pp. 1011-1013, 2004.

[4]   W. C. Nunnally, "Critical Component Requirements for Compact Pulse Power System Architectures," *Plasma Science, IEEE Transactions on,* vol. 33, pp. 1262-1267, 2005.

[5]   M. Gundersen, J. Dickens, and W. Nunnally, "Compact, portable pulsed power: physics and applications," in *Pulsed Power Conference, 2003. Digest of Technical Papers. PPC-2003. 14th IEEE International*, 2003, pp. 9-12 Vol.1.

[6]   E. Schamiloglu, K. H. Schoenbach, and R. J. Vidmar, "On the road to compact pulsed power: adventures in materials, electromagnetic modeling, and thermal management," in *Pulsed Power Conference, 2003. Digest of Technical Papers. PPC-2003. 14th IEEE International*, 2003, pp. 3-8 Vol.1.

[7]   C. Jiang, A. Kuthi, and M. A. Gundersen, "Toward ultracompact pseudospark switches," *Applied Physics Letters,* vol. 86, pp. 024105-3, 2005.

[8]   M. V. Fazio and H. C. Kirbie, "Ultracompact pulsed power," *Proceedings of the IEEE,* vol. 92, pp. 1197-1204, 2004.

[9]   H. M. Mott-Smith, "History of "Plasmas"," *Nature,* vol. 233, p. 219, 1971.

[10]   J. R. Roth, *Industrial Plasma Engineering* vol. 1. Bristol and Philedelphia: Instute of Physics Publishing, 1995.

[11]   E. Nasser, *Fundamentals of Gaseous Ionization and Plasma Electronics*: John Wiley & Sons, 1971.

[12]   A. Bogaerts, "The glow discharge: an exciting plasma," *Journal of Analytical Atomic Spectrometry,* vol. 14, pp. 1375-1384, 1999.

[13]   Y. P. Raizer, *Gas Discharge Physics*. Berlin: Springer, 1991.

[14]   G. Stockhausen and M. Kock, "Proof and analysis of the pendulum motion of beam electrons in a hollow cathode discharge," *Journal of Physics D: Applied Physics,* vol. 34, pp. 1683-1689, 2001.

[15]   H. Kirkici and D. Bruno, "Operating characteristics of a segmented hollow cathode over a wide pressure range," *Plasma Science, IEEE Transactions on,* vol. 23, pp. 229-234, 1995.

[16]   M. A. Gundersen and G. Schaefer, *Physics and Applications of Pseudosparks*. New York: Plenum Press, 1990.

[17]   F. Paschen, *Ann. Phys.,* vol. 37, p. 69, 1889.

[18]   K. Koppisetty and H. Kirkici, "Breakdown Characteristics of Helium and Nitrogen at kHz Frequency Range in Partial Vacuum for Point-to-Point Electrode Configuration," *In review,* 2007.

[19]   T. R. Burkes, "General Switching Considerations," in *Gas Discharge Closing Switches*. vol. 2, G. Schafer, M. Kristiansen, and A. Guenther, Eds. New York: Plenum Press, 1990, pp. 1-13.

[20]   G. Schaefer, M. Kristiansen, and A. Guenter, *Gas Discharge Closing Switches* vol. 2. New York: Plenum Press, 1990.

[21]   M. A. Gundersen, "Gas-phase pulsed power switches," *Plasma Science, IEEE Transactions on,* vol. 19, pp. 1123-1131, 1991.

[22]   W. C. Nunnally and A. L. Donaldson, "Self Breakdown Gaps," in *Gas Discharge Closing Switches*. vol. 2, G. Schaefer, M. Kristiansen, and A. Guenther, Eds. New York: Plenum Press, 1990, pp. 47-61.

[23]   I. Langmuir, "The Interaction of Electron and Positive Ion Space Charges in Cathode Sheaths," *Physical Review,* vol. 33, p. 954, 1929.

[24]   M. Gundersen, "Thyratrons," in *Gas Discharge Closing Switches*. vol. 2, A. Guenter and M. Kristiansen, Eds. New York: Plenum, 1990, pp. 375-378.

[25]   C. A. Pirrie and H. Menown, "The evolution of the hydrogen thyratron," 2000, pp. 9-16.

[26]   J. Creedon, "Design Principles and Operation Characteristics of Hydrogen Thyratrons," in *Gas Discharge Closing Switches*
vol. 2, G. Schaefer, A. Guenter, and M. Kristiansen, Eds. New York: Plenum Press, 1990.

[27]   J. Christiansen, "The Pseudospark Switch," in *Gas Discharge Closing Switches*. vol. 2 New York: Plenum Press, 1990.

[28]   J. Christiansen and C. Schultheiss, "Production of high current particle beams by low pressure spark discharges," *Zeitschrift für Physik A Hadrons and Nuclei,* vol. 290, pp. 35-41, 1979.

[29]   J. Christiansen and W. Hartmann, "The Pseudospark," in *Gas Discharge Closing Switches*. vol. 2, G. Schaefer, M. Kristiansen, and A. Guenther, Eds. New York: Plenum, 1990, pp. 509-519.

[30]   H. Riege and E. P. Boggasch, "High-power, high-current pseudospark switches," *Plasma Science, IEEE Transactions on,* vol. 17, pp. 775-777, 1989.

[31]   K. Frank and J. Christiansen, "The fundamentals of the pseudospark and its applications," *Plasma Science, IEEE Transactions on,* vol. 17, pp. 748-753, 1989.

[32]   M. Stetter, P. Felsner, J. Christiansen, K. Frank, A. Gortler, G. Hintz, T. Mehr, R. Stark, and R. Tkotz, "Investigation of the different discharge mechanisms in pseudospark discharges," *Plasma Science, IEEE Transactions on,* vol. 23, pp. 283-293, 1995.

[33]   W. Hartmann and G. Lins, "The spatial and temporal development of pseudospark switch plasmas," *Plasma Science, IEEE Transactions on,* vol. 21, pp. 506-510, 1993.

[34]   R. Stark, O. Almen, J. Christiansen, K. Frank, W. Hartmann, and M. Stetter, "An investigation of the temporal development of the pseudospark discharge," *Plasma Science, IEEE Transactions on,* vol. 23, pp. 294-299, 1995.

[35]   K. Frank, E. Boggasch, J. Christiansen, A. Goertler, W. Hartmann, C. Kozlik, G. Kirkman, C. Braun, V. Dominic, M. A. Gundersen, H. Riege, and G. Mechterscheimer, "High-power pseudospark and BLT switches," *Plasma Science, IEEE Transactions on,* vol. 16, pp. 317-323, 1988.

[36]   G. Kirkman and M. Gundersen, "The Back-Lighted Tyhratron," in *Gas Discharge Closing Switches*. vol. 2, G. Schaefer, M. Kristiansen, and A. Guenther, Eds. New York: Plenum Press, 1990, pp. 531-541.

[37]   C. Kozlik, K. Frank, O. Almen, J. Christiansen, A. Gortler, W. Hartmann, A. Tinschmann, and R. Tkotz, "Triggered low-pressure pseudospark-based high power switch," *Plasma Science, IEEE Transactions on,* vol. 17, pp. 758-761, 1989.

[38]   A. Gortler, J. Christiansen, R. Dotzer, and K. Frank, "Investigations of pulsed surface flashovers for the triggering of pseudospark high-power switches," *Plasma Science, IEEE Transactions on,* vol. 17, pp. 762-765, 1989.

[39]   V. D. Bochkov, V. M. Dyagilev, V. G. Ushich, O. B. Frants, Y. D. Korolev, I. A. Sheirlyakin, and K. Frank, "Sealed-off pseudospark switches for pulsed power applications (current status and prospects)," *Plasma Science, IEEE Transactions on,* vol. 29, pp. 802-808, 2001.

[40]   K. Higuchi, T. Shimada, M. Itagaki, T. Sato, and Y. Abe, "Effects of Electrode Geometry and Gas Pressure on Breakdown Voltage of a Pseudospark Discharge." vol. 35: The Institute of Pure and Applied Physics (IPAP), 1996, pp. 6259-6264.

[41]   K. K. Sozer E. B., Kirkici K. , "Pulsed Hollow Cathode Discharge Characteristics," in *IEEE Pulsed Power and Plasma Science Conference* 2007.